frontiers | Frontiers in Microbiology

TYPE Original Research
PUBLISHED 11 August 2025
DOI 10.3389/fmicb.2025.1649750

OPEN ACCESS

EDITED BY
Xiaoli Yu,
Southern Ocean Science and Engineering Guangdong Laboratory (Zhuhai), China

REVIEWED BY
Feng Huang,
Guangdong Academy of Agricultural Sciences, China
Susmita Das Nishu,
Ahsanullah University of Science and Technology, Bangladesh

*CORRESPONDENCE
Romy Chakraborty
✉ rchakraborty@lbl.gov

†These authors have contributed equally to this work

RECEIVED 18 June 2025
ACCEPTED 18 July 2025
PUBLISHED 11 August 2025

CITATION
Yadav A, Chen M, Acharya SM, Kim G, Yang Y, Zhao TZ, Tsang E and Chakraborty R (2025) A stable 15-member bacterial SynCom promotes *Brachypodium* growth under drought stress.
Front. Microbiol. 16:1649750.
doi: 10.3389/fmicb.2025.1649750

A stable 15-member bacterial SynCom promotes *Brachypodium* growth under drought stress

Archana Yadav[1†], Mingfei Chen[1†], Shwetha M. Acharya[1], Grace Kim[2], Yuguo Yang[1], Tiffany Z. Zhao[1], Eunice Tsang[1] and Romy Chakraborty[1*]

[1]Climate and Ecosystem Sciences Division, Earth & Environmental Sciences Area, Lawrence Berkeley National Laboratory, Berkeley, CA, United States, [2]Department of Molecular and Cell Biology, University of California Berkeley, Berkeley, CA, United States

Introduction: Rhizosphere microbiomes are known to drive soil nutrient cycling and influence plant fitness during adverse environmental conditions. Field-derived robust Synthetic Communities (SynComs) of microbes mimicking the diversity of rhizosphere microbiomes can greatly advance a deeper understanding of such processes. However, assembling stable, genetically tractable, reproducible, and scalable SynComs remains challenging.

Methods: Here, we present a systematic approach using a combination of network analysis and cultivation-guided methods to construct a 15-member SynCom from the rhizobiome of *Brachypodium distachyon*. This SynCom incorporates diverse strains from five bacterial phyla. Genomic analysis of the individual strains was performed to reveal encoded plant growth-promoting traits, including genes for the synthesis of osmoprotectants (trehalose and betaine) and Na^+/K^+ transporters, and some predicted traits were validated by laboratory phenotypic assays.

Results: The SynCom demonstrates strong stability both *in vitro* and *in planta*. Most strains encoded multiple plant growth-promoting functions, and several of these were confirmed experimentally. The presence of osmoprotectant and ion transporter genes likely contributed to the observed resilience of *Brachypodium* to drought stress, where plants amended with the SynCom recovered better than those without. We further observed preferential colonization of SynCom strains around root tips under stress, likely due to active interactions between plant root metabolites and bacteria.

Discussion: Our results demonstrate that trait-informed construction of synthetic communities can yield stable, functionally diverse consortia that enhance plant resilience under drought. Preferential colonization near root tips points to active, localized plant–microbe signaling as a component of stress-responsive recruitment. This stable SynCom provides a scalable platform for probing mechanisms of plant-microbe interaction and for developing microbiome-based strategies to improve soil and crop performance in variable environments.

KEYWORDS

microbiome, rhizosphere, *Brachypodium*, drought, SynCom, plant growth promotion (PGP)

Introduction

It is widely acknowledged that root-associated microorganisms play a crucial role in plant health and productivity. Root microbiomes aid plants by promoting nutrient acquisition (Mendes et al., 2013), producing plant growth hormones (Dodd et al., 2010; Eichmann et al., 2021), and conferring resilience under abiotic stresses such as drought and increase in salinity (Layeghifard

et al., 2017; Schmitz et al., 2022) among other beneficial functions. Plants recruit these root microbiomes primarily through the secretion of root exudates, that include organic acids, amino acids, nucleotides, vitamins, and fatty acids (Kawasaki et al., 2016; Zhalnina et al., 2018; Berendsen et al., 2018), orchestrating over time the structure of their root-associated microbiome (Voges et al., 2019; Pascale et al., 2019).

Numerous studies have emphasized the importance of root microbiomes (Bulgarelli et al., 2015; Liu et al., 2021), and have shown that specific microbial groups play a more crucial role than others (Gkarmiri et al., 2017; Bergelson et al., 2019). However, despite recent advancements in the field, identifying and selecting beneficial root microbes for applications in crop improvement continues to remain challenging, since a holistic understanding of the complex interactions between microbes and their host plants is still lacking (Finkel et al., 2017; Diwan et al., 2022; Kimotho and Maina, 2024). One promising approach involves constructing simplified synthetic communities (SynComs) derived from the root microbiome, where individual microbial strains co-exist, interacting with one another (Gupta et al., 2021; Shayanthan et al., 2022). Defined SynComs enable deeper understanding of how microbes cooperate, compete, and influence each other and the plant host in the rhizosphere ecosystem (de Souza et al., 2020), and allow designing targeted experiments to generate defensible hypotheses about role of microbial communities during plant growth and health under myriad environmental conditions. SynComs are typically constructed using either a reductionist approach or holistic approach. The reductionist approach relies on cultivation-based techniques, where microbes are isolated and cultured in the laboratory for study (Vorholt et al., 2017; Rodríguez Amor and Dal Bello, 2019; Liu et al., 2019; Xia et al., 2020). In contrast, the holistic approach assembles SynComs based on key microbial interactions observed in natural environment using culture-independent techniques like high-throughput sequencing (Zegeye et al., 2019; Gonçalves et al., 2023) However, both approaches have limitations. The reductionist approach often excludes key uncultivable microbes or assembles strains that do not originate from the rhizosphere microbiome, and therefore have genotypic and functional differences compared to microbes naturally present in rhizosphere soil (Liu et al., 2019). In contrast, the holistic approach relies heavily on genome sequencing, fails to differentiate between active or inactive bacteria—potentially leading to inaccurate diversity estimates—and assumes that the presence of genomic signatures directly correlates with functional activity (Gupta et al., 2021; Gutleben et al., 2018). These limitations highlight the need for an integrative strategy to construct SynComs that better mimic natural microbe-microbe and microbe-plant interactions (Chodkowski and Shade, 2017; McCarty and Ledesma-Amaro, 2019).

For broader applicability, it is desirable that a SynCom is stable (with robust colonization and prevalence throughout plant development), effective (able to confer beneficial traits to plants), and reproducible (yield consistent results across laboratory experiments). However, the successful assembly of such SynComs has been limited to a handful of prior reports (Shayanthan et al., 2022; McCarty and Ledesma-Amaro, 2019). In addition, only a few studies (Sanchez-Gorostiaga et al., 2018; Toju et al., 2020; Kabir et al., 2024) have demonstrated the persistence of introduced SynCom members in the rhizosphere, highlighting a critical gap in understanding their long-term functionality. Also, there is a growing interest in exploring the ability of rhizosphere microbiomes to alleviate drought stress in host plants observeable through declining crop production (Orimoloye, 2022; Tp, 2023; Seleiman et al., 2021). Similarly, poor agricultural practices like high-salinity irrigation is leading to salt stress, further intensifying crop yield losses (Atta et al., 2023). As a result, developing effective and stable SynComs—particularly those that enhance plant resilience under these stress conditions has emerged as a key focus in recent research. Syncoms offer a natural and sustainable alternative to over-reliance on chemical fertilizers for improving crop productivity (Shayanthan et al., 2022; Hao et al., 2021), though they have been addressed in only a limited number of studies (Schmitz et al., 2022; Flores-Duarte et al., 2023).

In this study, we hypothesize that a carefully designed and assembled SynCom, derived from the naturally grown *Brachypodium* rhizobiome, can enhance and support plant growth during environmental stress of drought and increased salinity. Using a combinatorial approach, we integrated culture-independent rhizobiome community analysis with network analysis to uncover critical microbe-microbe interactions. We then used culture-dependent methods to isolate key highlighted microbial strains, ultimately constructing a 15-member SynCom. We tested the stability and effectiveness of this SynCom. Genomic and phenotypic characterization of individual strains confirmed presence of plant-growth-promoting traits, and the SynCom's persistence was demonstrated when grown in planta. To further evaluate its effectiveness, we amended *Brachypodium* seedlings with the SynCom and subjected them to salinity and drought stresses. Using 16S amplicon sequencing, whole genome sequencing, assays for plant-growth-promoting traits, and plant phenotyping, we investigated correlations between plant phenotypes, SynCom abundance, and the SynCom's beneficial effects under these stress conditions. Finally, we examined the spatial distribution of SynCom strains on roots to determine whether they preferentially colonize specific root niches, providing insights into plant-microbe interactions under stress.

Materials and methods

Microbial isolation and identification

The 15-member SynCom was created using results from two interconnected experiments. In the first study (Acharya et al., 2023b), the microbe recruitment along the root surface was studied in young *Brachypodium* plants grown in natural soil. In the subsequent study (Chen et al., 2024), over 750 stable reduced community consortia (RCC) were enriched by growing root-attached microbes from the previous study over either 3 or 7 days in media with carbon substrates generally present in *Brachypodium* root exudates. In this study, based on high species diversity as denoted by the richness and Shannon diversity index, enrichments grown on two media, i.e., 0.1X R2A (BD Diagnostics), and RCH2 minimal media (Chakraborty et al., 2017) supplemented with carbon sources (either Glutamine or mixed carbon), were used to isolate colonies on the corresponding agar media plates by incubating the plates at 30°C in the dark for 7 days. Morphologically distinct colonies were picked and streaked for further purification. For species identification of the isolates, genomic DNA extracted using a PureLink Genomic DNA Mini Kit (Invitrogen, United States), was amplified using the universal 16S rRNA eubacterial primer pairs, i.e., 8F/27F and 1492R. DNA sequencing was carried out at the UC Berkeley DNA Sequencing Facility. Geneious Prime

v2020.2.5 was used to process the 16S reads and the resulting consensus sequences were taxonomically classified using the SILVA database (Gurevich et al., 2013).

Genomic analysis of individual isolates

The whole genome sequencing was performed at Novogene (Illumina Novaseq 6,000 platform). Genome assembly and annotation were performed using the KBase platform (Arkin et al., 2018). Raw reads quality was assessed with FastQC v0.11.9, followed by trimming using Trimmomatic v0.36 (Bolger et al., 2014). The reads were then assembled using Spades v3.15.3 (Prjibelski et al., 2020) and the genome quality was evaluated using CheckM v1.0.18 (Parks et al., 2015). DRAM v0.1.2 (Shaffer et al., 2020) and Blastkoala (Kanehisa et al., 2016) were used to assign KEGG orthology (KO) numbers and functional annotation to the protein-coding genes and KEGG mapper (Kanehisa and Sato, 2020) was used to visualize metabolic pathways. Annotations from the metabolic assembly output files obtained from DRAM and KEGG were used to search for specific properties or genes such as PGP traits, transporters, and osmoprotectant-related genes. For the taxonomic classification, a concatenated alignment of 120 single-copy marker proteins was created using the GTDB-tk workflow (Parks et al., 2022; Chaumeil et al., 2022). Subsequently, 4–5 representative sequences closest to the SynCom strains were selected and aligned using clustalo (Sievers et al., 2011). This was followed by the tree construction with FastTree (Price et al., 2009) and visualization using iTOL (Letunic and Bork, 2007).

Testing persistence of SynCom members under *in vitro* conditions

We evaluated *in vitro* stability of the 15-member SynCom by tracking changes in the relative abundances of the strains over a three-week period. For this, we cultured 5 mL of the inoculum, containing equal cell numbers (4×10^7 cells) of each SynCom member, in 45 mL of 0.2X MS (Murashige and Skoog) media (M0404, Sigma Aldrich, United States). The mixture was incubated in a plant growth chamber with conditions set at 16-h light, 24°C temperature, and 50% humidity. At the end of each week, 5 mL of the culture was transferred to 45 mL of fresh 0.2X MS media, and 5 mL of the culture was sampled for 16S rRNA community analysis.

Seed germination and preparation of inoculum for in planta experiments

Approximately 150 *Brachypodium distachyon* (Bd 21–3) seeds were dehusked and sterilized by following the procedures as described in the protocol (Novak et al., 2024). Seeds were immersed in 70% ethanol for 30 s, 50% bleach for 5 min, and then washed five times with autoclaved MQ water. The sterilized seeds were stored in sterile water at 4°C in the dark for 1 week. Subsequently, the seeds were germinated on semisolid plates containing 0.5X MS media with 0.4% w/v phytagel and placed in a plant growth chamber (Percival Scientific AR-41 L3, United States) set to 16 h of light, 24°C temperature, and 50% humidity for 3–5 days (Ingram et al., 2012; Li et al., 2019). For potting, sterilized plastic pots (3.9”D x 3.94” W x 3.15” H, Manufacturer: MiMiLai) lined with coffee filters and filled with autoclaved calcined clay (PROFILE Products LLC, United States) were used. The clay was saturated with 0.2X MS media before transplanting one seedling per pot. The weight of each pot, once filled with clay and plants and watered to clay saturation, was recorded as the saturation weight.

Individual SynCom isolates were cultivated in R2A media for 24–72 h until they reached log phase (Supplementary Figure S8). After cultivation, the isolates were checked for purity, washed three times, and resuspended in a 30 mM phosphate buffer. For each isolate suspension, cells were stained with the nucleic acid stain SYBR green and counted using a flow cytometer (AttuneNxT®, ThermoFisher Scientific) following the manufacturer's instructions. Suspensions for individual isolates were adjusted to equal cell numbers, specifically 4.1×10^7 cells, for the final inoculum used in subsequent *in planta* experiments.

Assessing the performance of SynCom under drought and salinity stress

This experiment comprised three conditions: Drought, Rewatered drought, and Salinity, to reflect natural environmental stresses. Each condition included two experimental sets; (1) SynCom-amended plants where 1 mL of 30 mM phosphate buffer containing equal cell numbers of each SynCom strain were inoculated at the base of plant shoot 3 days before inducing stress conditions, and (2) unamended plants where 1 mL of 30 mM phosphate buffer was inoculated at the base of plant shoot 3 days before inducing stress conditions. Each experimental set contained 7 plant replicates. After transplanting seedlings into pots, they were watered with 0.2X MS media to maintain 80% saturation weight for 4 days, after which they were inoculated with either SynCom or buffer, as explained earlier.

In addition to the three stress conditions, there was a control set with both SynCom-amended and unamended plants, maintained at 80% saturation weight by watering with 0.2X MS media. Stress induction began 3 days after SynCom inoculation. The 'Drought' condition involved maintaining plants at 40% saturation weight (Gombos et al., 2023) by watering with 0.2X MS media until they were harvested 21 days after stress induction. The 'Rewatered drought' condition involved 14 days of drought treatment, followed by restoring saturation weight to 80% for the last week before harvest. The 'Salinity' condition involved watering the plants at 80% saturation weight with 0.2X MS media containing 60 mM NaCl. All these plants were incubated in a plant growth chamber (Percival Scientific AR-41 L3, United States) set to 16 h of light, 24°C temperature, and 50% humidity. After 3 weeks of stress induction, plants were harvested by gently removing them from the pots for phenotypic measurements, including shoot wet weight, root length, leaf count, and shoot length (longest leaf). In addition, root tip and root base samples were aseptically harvested as 2 cm cuttings and suspended in 5 mL of 5 mM sodium pyrophosphate + 30 mM phosphate buffer. The sample was sonicated for 10 min and subsequently left on a benchtop for 5 min to allow soil particles to settle down. The supernatant was pipetted out and pelleted to collect microbial cells. DNA extracted from these samples were sent to Novogene, United States, for amplicon sequencing. Quantitative Insights Into Microbial Ecology (QIIME2; Bolyen et al., 2019) was used to process 16S rRNA amplicon data. Within QIIME2, DADA2 was employed for quality filtering, chimera checking, and paired-end read joining. The resulting sequences were trimmed to obtain V4

region (515F-806R), and taxonomic classification was performed using the SILVA database (Quast et al., 2013).

Assay for plant growth promoting traits in the SynCom strains

Indole-3-Acetic Acid (IAA) assay: The protocol for IAA assay was adapted from Gilbert et al. (2018). Briefly, the isolates were cultured in 5 mL R2A media, with and without 0.5 mg/mL L-tryptophan, for 3 days at 30°C. Following incubation, cultures were centrifuged at 14,000 rpm for 5 min, and 100 µL supernatant was transferred to a 96-well microplate. Subsequently, 200 µL of Salkowski reagent (2% of 0.5 M $FeCl_3$ in a 35% $HClO_4$ solution) was added to each well. IAA standards (0–10 µg/mL) were also prepared simultaneously. The microplate was incubated in the dark for 30 min, and absorbance values at OD_{530} was recorded to quantify IAA production using the standard curve.

ACC-deaminase activity: The method for measuring 1-Aminocyclopropane-1-carboxylate (ACC) deaminase production in bacterial isolates was adapted from the colorimetric ninhydrin assay described by Li et al. (2011). Briefly, SynCom isolates were cultivated in 2 mL of DF salinity minimum media supplemented with 3 mM ACC for 24 h. Following incubation, 1 mL of the culture was centrifuged at 8,000 x g for 5 min. Subsequently, 100 µL of the resulting supernatant was diluted tenfold, and the ninhydrin assay, with ACC standards ranging from 0.5 mM to 0.005 mM, was used to quantify bacterial ACC consumption.

Phytate solubilization assay: Isolates were inoculated into 3 mL of filter-sterilized phytase-specific medium (PSM; Hosseinkhani and Hosseinkhani, 2009) supplemented with 0.5 mM of Sodium phytate (Fisher Scientific). The cultures were then incubated for 48 h at 30°C in a shaker incubator set at 80 rpm. Following incubation, the OD_{600} was measured, and the cultures were centrifuged at 10,000 rpm for 15 min. The resulting supernatant was retained for a colorimetric assay using the QuantiChrom™ Phosphate Assay Kit (BioAssay Systems, CA, United States). Absorbance was measured at 620 nm and compared against the provided phosphate standards included with the Phosphate Assay Kit.

Siderophore production assay: The capability of siderophore production by the isolates was assessed using the CAS overlaying medium assay (Acharya et al., 2023a; Louden et al., 2011; Pérez-Miranda et al., 2007). Briefly, each isolate was cultured on R2A agar plates at 30°C for 3 days. Subsequently, blue CAS medium with 0.9% agar was overlaid onto the plates. The plates were then further incubated in the same conditions and monitored for color changes over an additional 4 days. The presence of a yellow halo surrounding colonies indicated positive siderophore production. As a positive control, *Burkholderia* sp. PA-E8, a known siderophore producer isolated at our laboratory, was included (Darling et al., 1998; Ong et al., 2016).

Biofilm formation assay: The crystal violet assay for quantifying biofilm formation was adapted from Haney et al. (2021). Briefly, each isolate was grown in R2A media, washed, and resuspended in a 30 mM phosphate buffer to a final OD_{600} of 0.2. The cultures were inoculated into 96-well microtiter plates containing 180 µL of 0.2X MS media, at a 1:10 (v/v) ratio to achieve a final volume of 200 µL (initial OD_{600} of 0.02). The plates were incubated statically at 30°C for 3 days. Post incubation, the liquid fraction was removed by inverting the plates, and each well was washed three times with MilliQ water and air-dried. Subsequently, 100 µL of a 0.1% crystal violet solution (0.1% v/v crystal violet, 1% v/v methanol, and 1% v/v isopropanol in MilliQ water) was added to each well, followed by a 30-min incubation at room temperature. After discarding the staining solution, wells were rinsed three times with MilliQ water. Biofilms were destained with 100 µL of a 30% acetic acid solution and incubated at room temperature for 30 min. OD_{595} of the destaining solution was measured for biofilm quantification.

Gibberellin (GA) assay: The protocol for gibberellin quantification was adapted from Graham and Henderson (1961). Briefly, microbial isolates were cultured in R2A broth at 30°C for 48 h until they reached late-log phase. Cultures were centrifuged at 8,000 rpm for 5 min, and the supernatant was acidified to pH 1.5–2.0 using HCl. An equal volume of ethyl acetate was added, mixed thoroughly, and allowed to separate into organic and aqueous layers. The upper ethyl acetate layer, containing gibberellins, was collected and extracted twice. Combined extracts were vortexed to homogenize, and 50 µL was mixed with 750 µL phosphomolybdic acid reagent in 2 mL tubes. Samples were incubated in a boiling water bath for 1 h, cooled to room temperature, and 200 µL was transferred to a 96-well microplate for absorbance measurement at 780 nm. Gibberellin concentrations were determined using a standard curve prepared from 0 to 10 mg/mL gibberellic acid in absolute alcohol, processed alongside samples.

Acid and Alkaline Phosphatase assay: The protocol for assessing acid and alkaline phosphatase activity was adapted from Sinsabaugh (2001) and Allison (2007). Microbial isolates were cultivated in phytate minimal medium at 30°C until reaching mid-log phase. Cultures were then subjected to OD600 measurements and centrifuged at 8,000 rpm for 5 min. The supernatant was discarded, and the cell pellets were washed three times with, and subsequently resuspended in, 50 mM boric buffer (pH 9) for alkaline phosphatase assays or 50 mM acetate buffer (pH 5) for acid phosphatase assays. For each assay, 750 µL of the cell suspension was mixed with 750 µL of 5 mM p-nitrophenyl phosphate (pNPP) prepared in the corresponding buffer. A substrate control was prepared by combining 750 µL of 5 mM pNPP with 750 µL of buffer alone. All reactions, including isolate samples and controls, were incubated at room temperature for 45 min. Following incubation, samples were centrifuged at 10,000 rpm for 1–2 min. A 750 µL aliquot of the resulting supernatant was transferred to a fresh tube, and 75 µL of 1.0 M NaOH was added to terminate the reaction and facilitate color development. A 300 µL portion of this solution was then transferred to a 96-well microplate, and absorbance was measured at 410 nm. Phosphatase activity was quantified by comparing absorbance values to a standard curve of p-nitrophenol prepared in the corresponding buffer.

Carbon source utilization assay: Each isolate's growth was assessed on 18 *Brachypodium* root-exudate carbon sources that are significantly enriched during drought stress (Skalska et al., 2021; Fisher et al., 2016; Ahkami et al., 2019; Supplementary Table S2). Cultures were incubated aerobically in 0.2 × MS medium supplemented with 5 mM of each carbon source at 30°C in the dark, with shaking, in biological triplicate. Cell density (OD600) was recorded at 0, 24, 48, 92, 120, 144, and 168 h. The growth was considered positive when the OD600 increased by more than 0.07 relative to the 0-h measurement.

Statistical analyses

Network analysis and SynCom member interactions: To understand the interspecies interactions from 0.1X R2A enrichments which have the highest diversity and most isolates, the top 50 most abundant ASVs among the core ASVs (present in >75% samples from the 4 generations) from this enrichment were selected. Their abundance matrix across all samples was analyzed using "NetCoMi" package (Peschel et al., 2021) in R. Pearson correlation coefficients greater than 0.3 and Student's t-test results with p-values less than 0.05 were used to generate a sparse matrix for the network analysis. In the correlation network, each node represents an individual ASV, with different colors representing the corresponding modules. The edges connecting the nodes indicate a strong and significant correlation between the ASVs. The clustering in this network was used to group ASVs into modules that are densely interconnected internally but have sparse connections with other modules.

SynCom strain abundances in the rhizosphere under drought and salinity stress: To identify the changes in individual SynCom member's abundances under stress, natural log fold differences between the control versus drought, rewatered drought, and salinity conditions were assessed using Analysis of Compositions of Microbiomes with Bias Correction (R package "ANCOMBC"; Lin and Peddada, 2020; Martins et al., 2023). False discovery rates were controlled using the Benjamini-Hochberg method.

Rhizosphere functional redundancy of SynCom members in stress conditions: To test whether the plants under stress modulate rhizosphere microbiome toward similar functions, functional redundancy (FR) across different environments (de Bello et al., 2021) estimated and compared using the R package "SYNCSA" (Debastiani and Pillar, 2012).

Results

Selection of isolates to construct a 15-member SynCom

In our previous research, we had developed a number of reduced-complexity microbial enrichments from the rhizosphere of *Brachypodium distachyon* (Chen et al., 2024). We isolated 175 bacterial strains from those enrichments, which we classified by their 16S rRNA genes using the SILVA database (Pruesse et al., 2012). These isolates represented six phyla: Alphaproteobacteria (15), Gammaproteobacteria (124), Actinobacteria (15), Firmicutes (13), Bacteroidetes (7), and Acidobacteria (1).

Out of those isolates, we downselected 15 isolates that showed a 100% match in their 16S rRNA gene sequences with both top abundant ASVs from these enrichments (Chen et al., 2024) and with sequences from their rhizosphere origins (Acharya et al., 2023b). To build a SynCom that is truly representative of the *Brachypodium* rhizosphere microbiome, we considered the following criteria: (1) relative abundance of different microbial taxa within the enrichments, (2) representation of phylogenetic diversity among the most abundant microbes, and (3) network interactions among the taxa. Together, the ASVs corresponding to these 15 isolates made up 79.93% of the total reads in the enrichments. We also conducted network analyses on the top 50 ASVs to identify key interactions, which revealed six distinct modules (Figure 1) and a total of 38 positive and 17 negative correlations—24 positive and 9 negative of which occurred among our SynCom members. For the ASVs that matched with selected isolates, six were in Module 1, five in Module 3, three in Module 4, and two each in Modules 5 and 6, which cover most network modules. Some isolates, like *Mesorhizobium* sp. RCC-202 (degree = 8) and *Leifsonia* sp. RCC-180 (degree = 5), showed high network degrees (number of significant correlations connecting to the node), suggesting they play important roles in maintaining network structure. All but one strain, *Bosea* sp. RCC-152.1, had positive connections with at least one other strain across different modules. Informed by all these different analyses, we assembled a SynCom with these 15 isolates that represent taxonomically diverse 5 distinct bacterial phyla (Proteobacteria, Bacteroidota, Acidobacteriota, Actinobacteriota and Firmicutes; Figure 2).

Genomes of SynCom isolates encode multiple PGP traits

Genomic analysis of nearly complete genomes for all 15 isolates showed that they exhibited a wide range of genome sizes (3.7 Mbp − 8 Mbp), GC content (35–69%), and numbers of genes (3343–7,740). The key general genome features of the SynCom isolates are outlined in Table S1. Most SynCom isolates encoded either a complete set of genes or the essential genes involved in pathways known to be associated with PGP traits (Olanrewaju et al., 2021; Bruto et al., 2014; Gupta et al., 2014; Bhattacharyya and Jha, 2012), potentially contributing to overall plant growth (Table 1). Some of the important PGP traits encoded in the genomes of multiple isolates included 1-aminocyclopropane-1-carboxylate (ACC) deaminase production (9 isolates), Indole-3-acetic acid (IAA) for auxin synthesis (2 isolates), synthesis of antimicrobial compound, i.e., gamma-aminobutyric acid (GABA; 12 isolates), genes associated with plant hormones like amidases (13 isolates), synthesis of volatile organic compounds (VOCs) i.e., 2,3 butanediol and acetoin (14 isolates), trehalose synthesis (13 isolates) siderophore production or transportation (11 isolates), and EPS production (15 isolates; Table 1).

SynCom strains express multiple PGP traits during phenotypic characterization

We tested eight PGP traits essential for plant's growth by conducting phenotypic assays. These include IAA production, ACC deaminase activity, phytate solubilization, siderophore production, biofilm formation, Gibberellin production, and Acid and Alkaline Phosphatase assay (Table 2). Six SynCom isolates produced IAA in the presence of L-tryptophan, with concentrations ranging from 0.25 to 23 µg/mL. The highest IAA levels (~23 µg/mL) were observed in *Enterobacter* sp. RCC-40 and *Mucilaginibacter* sp. RCC-168. All SynCom isolates exhibited ACC deaminase activity, with nine strains degrading more than 50% of the supplied 3 mM ACC. Siderophore production was detected in seven isolates, indicated by the formation of a yellow halo in the o-CAS assay (Table 2). Ability to form biofilms, as assessed by crystal violet assay, was significant (p-value < 0.05) by Student's t-test in nine isolates. All the isolates produced Gibberellins, with Bacillus sp. RCC-6.1 and Enterobacter sp. RCC-40 showing the highest levels. Five

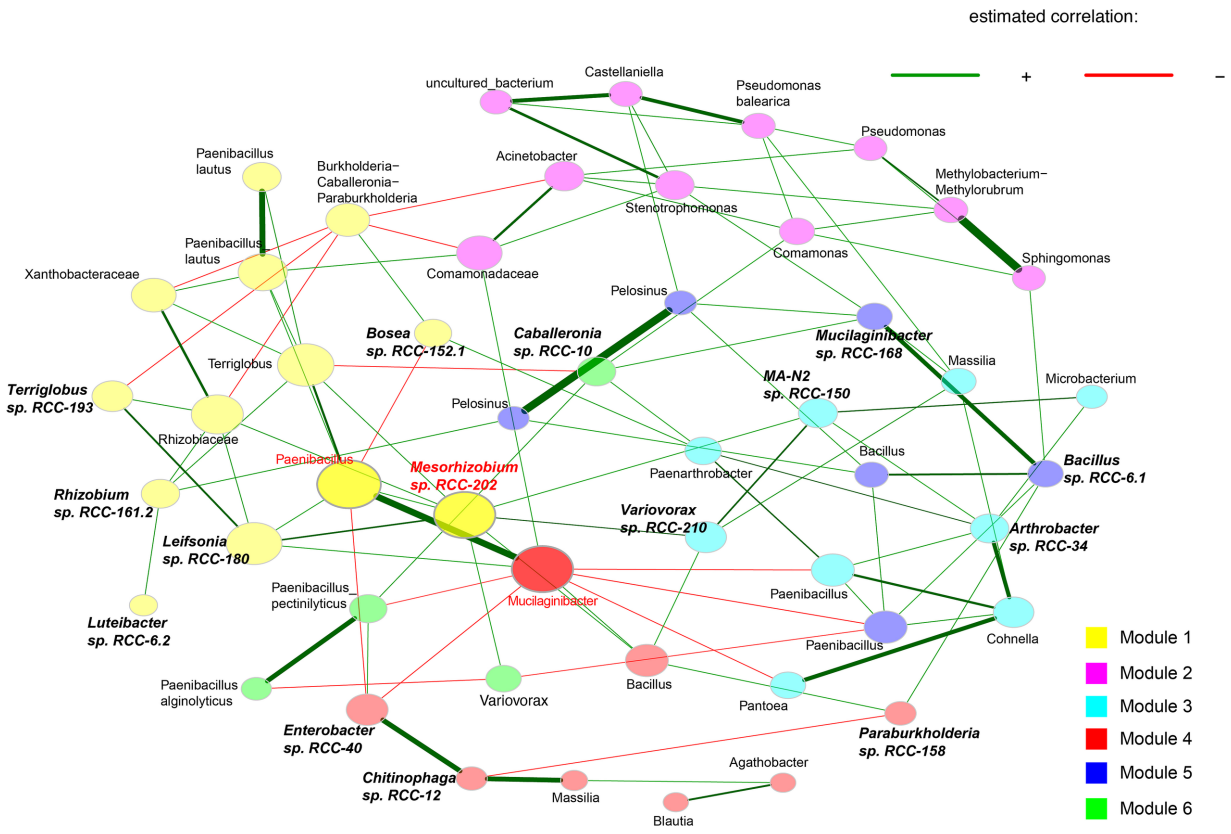

FIGURE 1
Association networks calculated using the 50 most abundant bacterial ASVs from 0.1X R2A enrichments. The abundance matrices from all samples were loaded into R to construct and visualize the network using the "NetCoMi" package. Networks were generated using the fast greedy clustering algorithm with a Pearson correlation coefficient threshold of ± 0.3, and a t-test (< 0.05) for sparse matrix generation. Eigenvector centrality is used for defining hubs and scaling node sizes. Positive correlations are displayed in green and negative in red. Shape color represents species clusters that are more likely to co-occur with one another than with species outside these modules. Hubs are highlighted in red with corresponding taxon names, whereas SynCom isolates have bolded and italicized names.

isolates, including *Luteibacter* sp. RCC-6.2, *Terriglobus* sp. RCC-193, *Mucilaginibacter* sp. RCC-168, *Leifsonia* sp. RCC-180, and *Rhizobium* sp. RCC-161.2, demonstrated phytate solubilization with phosphorus release in the range of 0.0003–0.006 mg/dL. Six isolates produced acid phosphatase, with Bosea sp. RCC-152.1 and Enterobacter sp. RCC-40 exhibited the highest activity (~600 uM), while the remaining isolates produced <200 uM. Lastly, five isolates produced alkaline phosphatase, with Enterobacter sp. RCC-40 and Arthrobacter sp. RCC-34 displaying the highest concentrations (146–375 uM; Table 2). Notably, *Mucilaginibacter* sp. RCC-168 tested positive for all eight PGP traits. We also evaluated each strain's growth on 18 drought-enriched *Brachypodium* exudates (Skalska et al., 2021; Fisher et al., 2016; Ahkami et al., 2019). Eleven of these compounds were metabolized by every isolate (Supplementary Figure S1). *Paraburkholderia* sp. RCC-158 grew on all 18 substrates and exhibited the most rapid growth as indicated by OD600 increase (Supplementary Figure S2).

SynCom strains exhibit better persistence in planta

Since all strains were isolated from the plant rhizosphere, we hypothesized that the presence of the plant host would positively impact SynCom growth and stability. To test this, we first examined SynCom growth by combining 15 strains in equal cell volumes and inoculating them into 0.2X MS media, which we generally used to water the plants. Samples were collected weekly, and community composition assessed through 16S rRNA (V3-V4 region) sequencing (Figure 3). The results showed that six of the 15 strains were undetectable or had a relative abundance below 0.1% after 3 weeks. Notably, the *in vitro* environment did not support the growth of Gram-positive strains, as three (*Arthrobacter* sp. RCC-34, *Leifsonia* sp. RCC-180, and *Bacillus* sp. RCC-6.1) of the four were either absent or present at very low abundance (<0.1%) when sampled. Conversely, members such as *MA-N2* sp. RCC-150, *Paraburkholderia* sp. RCC-158 and *Chitinophaga* sp. RCC-12, dominated the culture at the end of week 3 with an average relative abundance of 60, 26 and 8%, respectively (Figure 3).

Next, we evaluated the growth and persistence of SynCom members in the presence of *Brachypodium*. After 3 weeks of growth *in planta*, the relative abundance of strains was more evenly distributed (Figure 4B). Notably, Gram-positive strains such as *Arthrobacter* sp. RCC-34 (1.4%) and *Leifsonia* sp. RCC-180 (0.6%) showed substantial increases in relative abundance compared to *in vitro* conditions. In contrast, *Bacillus* sp. RCC-6.1, showed a low relative abundance (<0.1%). Additionally, 11 of the 15 strains displayed higher median relative abundances when grown with the plant than without (Supplementary Figure S3).

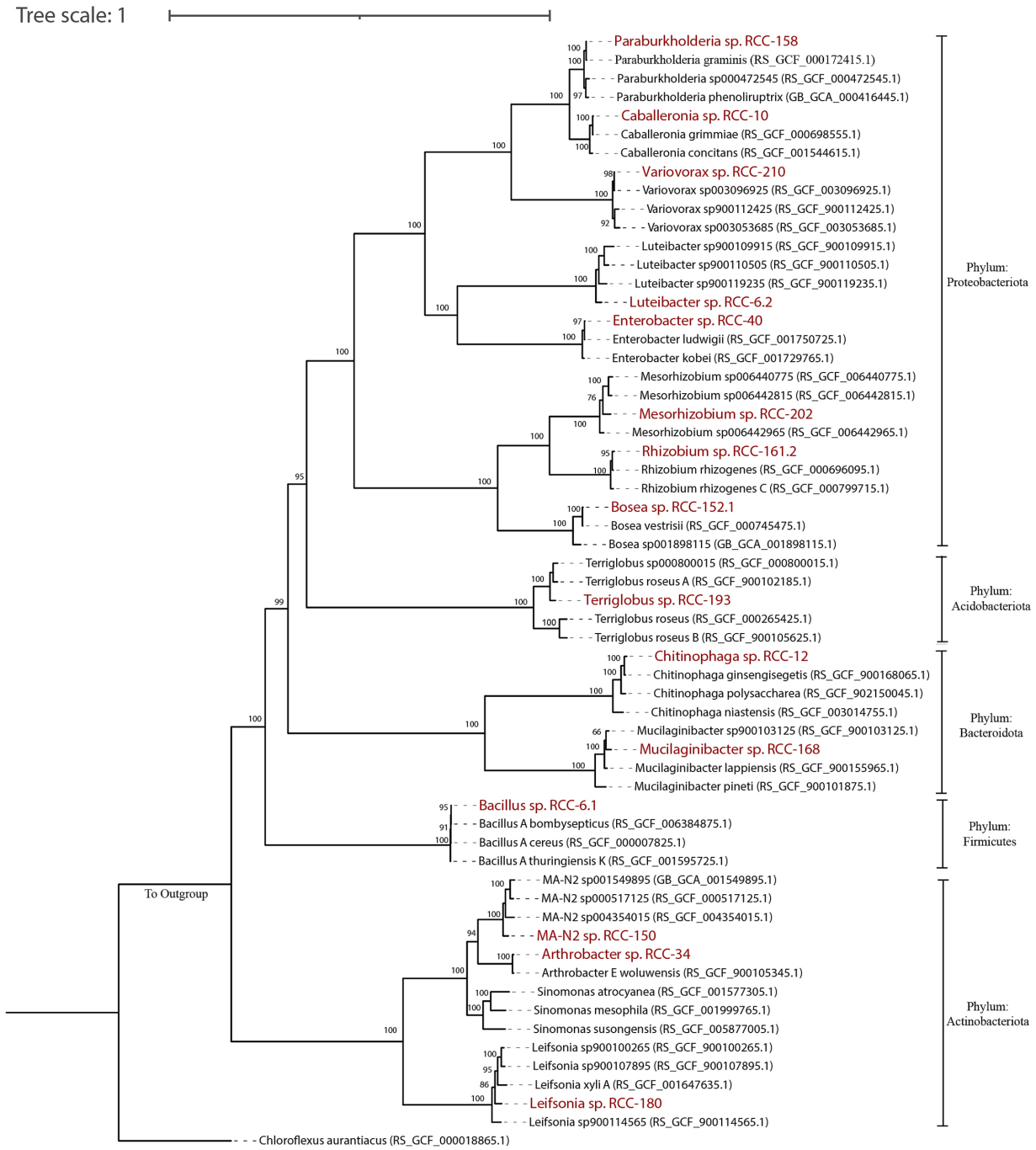

FIGURE 2
A phylogenomic tree for 15 SynCom isolates was constructed using multiple sequence alignment (MSA) from the concatenation of 120 marker proteins obtained via GTDB-tk workflow. The tree was visualized and edited using iTOL. To create the tree, 2–5 genomes closest to the SynCom isolates were included, with Genbank accession numbers in parentheses. The 15 SynCom members are highlighted in bold red. Phylum-level taxonomy for each genome is indicated on the right side of the tree. Bootstrap values (from 100 replicates) are displayed for nodes over 40 bootstrap supports. *Chloroflexus auranticus* was used as an outgroup to root the tree.

Drought and salinity stress in *Brachypodium* enrich specific SynCom strains

We assessed the impact of the SynCom on plant phenotype under drought and salinity stress, two common environmental stressors that plants encounter. No significant differences were observed between SynCom-amended and unamended plants with regards to shoot height, shoot weight, root length, or leaf number under drought stress (Figure 4A; Supplementary Figure S7). However, SynCom-amended plants showed significant improvements across all these above measured parameters (t-test, Figure 4A) on rewatering after drought. Under salinity stress, SynCom-amended plants exhibited a significant increase in shoot height compared to unamended plants (Figure 5A).

TABLE 1 Plant growth promoting (PGP) traits genes encoded in genomes of SynCom isolates: the table categorizes genes according to their general Plant Growth Promoting Rhizobacteria (PGPR) functions (Column A), specific pathways (Column B), and the presence of these genes in the syncom member genomes (Column C).

Overall function as PGPR	Specific functions	Genes	*Caballeronia* sp. RCC-10	*Chitinophaga* sp. RCC-12	*MA-N2* sp. RCC-150	*Paraburkholderia* sp. RCC-158	*Rhizobium* sp. RCC-161.2	*Mucilaginibacter* sp. RCC-168	*Leifsonia* sp. RCC-180	*Terriglobus* sp. RCC-193	*Mesorhizobium* sp. RCC-202	*Variovorax* sp. RCC-210	*Arthrobacter* sp. RCC-34	*Enterobacter* sp. RCC-40	*Luteibacter* sp. RCC-6.2	*Bosea* sp. RCC-152.1	*Bacillus* sp. RCC-6.1
Plant hormones	Auxin	Auxin/IAA synthseis/ Indole-3-Butyric Acid (IBA is precursor for IAA) *ipdC(4.1.1.74)/ppdC* (indole-3-pyruvate decarboxylase/phenylpyruvate decarboxylase gene)	No	No	No	No	No	No	No	No	No	No	No	Yes	No	No	Yes
	Amidase	Amidase (*amiE*; K01426) [EC:3.5.1.4]	Yes	Yes	Yes	Yes	Yes	Yes	Yes	Yes	Yes	Yes	No	No	Yes	Yes	Yes
	Tryptophan	Tryptophan 2-monooxygenase (*iaaM*; K00466) [EC:1.13.12.3]	No	No	No	Yes	No	No	No	No	No	No	No	No	No	No	No
	Gibberllins	Geranylgeranyl diphosphate synthase (*ggps*) [EC:2.5.1.1]	No	No	Yes	No	No	No	Yes	Yes	No	Yes	Yes	No	No	No	Yes
		Diterpene synthases/cyclases (*cps/ks*) and Cytochrome P450 monooxygenases (cyp112/ cyp114/cyp117)	No	No	No	No	No	No	No	No	No	No	No	No	No	No	No
	Putresciene	Ornithine decarboxylase [EC:4.1.1.17] for putresciene synthesis	No	No	No	No	Yes	No	No	No	Yes	No	No	No	No	Yes	No
Stress response	γ-aminobutyric acid (GABA) production	glutamate decarboxylase gadA/B	No	No	Yes	No	No	No	Yes	No	No	No	Yes	No	No	No	Yes
		glutamate: GABA antiporter (gadC)	No	No	No	No	No	No	Yes	No	No	No	No	Yes	No	No	No
		γ-aminobutyric acid (GABA) gene *gabD* K00135 Succinate-semialdehyde dehydrogenase / glutarate-semialdehyde dehydrogenase	Yes	No	Yes	Yes	Yes	No	Yes	Yes	Yes	Yes	Yes	Yes	No	Yes	Yes
	Ubiquinone biosynthesis	ubiB	No	No	No	No	No	No	No	No	No	No	No	No	No	Yes	No
	Leucine catabolism	2-oxoisovalerate dehydrogenase [EC:1.2.4.4]	No	Yes	Yes	No	Yes	Yes	Yes	Yes	Yes	No	Yes	No	Yes	Yes	Yes
	Quorum sensing	*luxS EC 4.4.1.21 and lsrABCD both*	No	No	No	No	No	No	No	No	No	No	No	Yes	No	No	No
	Modulation of plant's ethylene level by Ethylene synthesis	ACC deaminases (1-aminocyclopropane-1-carboxylate deaminase [EC:3.5.99.7]) Alternative enzyme ([EC:4.4.1.15] dcyD)	Yes	Yes	No	Yes	Yes	Yes	No	No	Yes	Yes	No	Yes	No	Yes	No
	Asparagine utlization	Glutamin-(asparagin-)ase *(aspQ/ansAB).* 3.5.1.38	No	No	No	No	No	No	No	No	No	Yes	No	No	No	No	No

(Continued)

10.3389/fmicb.2025.1649750

TABLE 1 (Continued)

Overall function as PGPR	Specific functions	Genes	*Caballeronia* sp. RCC-10	*Chitinophaga* sp. RCC-12	*MA-N2* sp. RCC-150	*Paraburkholderia* sp. RCC-158	*Rhizobium* sp. RCC-161.2	*Mucilaginibacter* sp. RCC-168	*Leifsonia* sp. RCC-180	*Terriglobus* sp. RCC-193	*Mesorhizobium* sp. RCC-202	*Variovorax* sp. RCC-210	*Arthrobacter* sp. RCC-34	*Enterobacter* sp. RCC-40	*Luteibacter* sp. RCC-6.2	*Bosea* sp. RCC-152.1	*Bacillus* sp. RCC-6.1
	H2S production	*cysC K00860*	No	No	No	No	No	No	No	No	Yes	No	No	Yes	No	No	Yes
		cysJ K00380	No	No	No	No	No	No	No	Yes	No	No	No	Yes	No	No	No
		cysI K00381	Yes	No	No	Yes	Yes	No	No	No	Yes	Yes	No	Yes	No	Yes	No
		cysN K00956	Yes	Yes	Yes	Yes	Yes	Yes	No	Yes	Yes	Yes	Yes	Yes	No	Yes	No
	Biofilm formation	lpx genes for for lipid A biosynthesis from KEGG	Yes	Yes	No	Yes	Yes	Yes	No	Yes	Yes	Yes	No	Yes	Yes	Yes	No
		Curli related proteins	Yes	No	No	No	No	No	No	No	No	No	No	Yes	No	No	No
		pgaABCD poly-beta-1-6-N-acetylglucosamine synthesis protein	No	No	No	No	No	No	No	No	No	Yes	No	Yes	Yes	No	No
Volatile organic compounds (VOCs)	2,3 butanediol and acetoin Synthesis	Acetolactate synthase I/III small subunit (K01653)	Yes	Yes	Yes	Yes	Yes	Yes	Yes	Yes	Yes	Yes	Yes	Yes	Yes	Yes	Yes
		Acetolactate synthase I/II/III large subunit (K01652)	Yes	Yes	Yes	Yes	Yes	Yes	Yes	Yes	Yes	Yes	Yes	Yes	Yes	Yes	Yes
		Threonine 3-dehydrogenase (K00060) [EC:1.1.1.103]	Yes	Yes	Yes	Yes	Yes	Yes	Yes	No	Yes	No	Yes	Yes	Yes	No	Yes
		Acetolactate decarboxylase *budA* (K01575) [EC:4.1.1.5]	No	Yes	No	No	No	Yes	No	No	No	No	No	Yes	No	No	Yes
		(R, R)-butanediol dehydrogenase / meso-butanediol dehydrogenase / diacetyl reductase *budB* (K00004) EC:1.1.1.4 1.1.1.- 1.1.1.303	No	No	No	Yes	No	No	Yes	No	No	No	No	No	No	No	Yes
		Meso-butanediol dehydrogenase / (S, S)-butanediol dehydrogenase / diacetyl reductase *budC* (K18009) EC:1.1.1.304	Yes	No	No	Yes	Yes	No	No	No	No	Yes	Yes	Yes	No	Yes	No
Trehalose	Trehalose Synthesis	Trehalose 6-phosphate phosphatase (*otsB*; K01087) [EC:3.1.3.12]	Yes	No	Yes	Yes	Yes	No	Yes	No	Yes	Yes	Yes	Yes	Yes	Yes	No
		Trehalose 6-phosphate synthase/phosphatase (*otsA*; K16055) [EC:2.4.1.15 3.1.3.12]	Yes	Yes	Yes	Yes	Yes	Yes	Yes	No	Yes	Yes	Yes	Yes	Yes	No	No
		Maltooligosyltrehalose trehalohydrolase (*treZ*; K01236) [EC:3.2.1.141]	Yes	Yes	Yes	Yes	Yes	Yes	Yes	Yes	No	Yes	No	Yes	Yes	Yes	No
		(1- > 4)-alpha-D-glucan 1-alpha-D-glucosylmutase (*treY*; K06044) [EC:5.4.99.15]	Yes	Yes	Yes	Yes	Yes	Yes	Yes	Yes	No	Yes	No	Yes	Yes	Yes	No
		Maltose alpha-D-glucosyltransferase/ alpha-amylase (*treS*; K05343) [EC:5.4.99.16 3.2.1.1]	Yes	No	Yes	Yes	Yes	No	Yes	Yes	No	Yes	Yes	Yes	Yes	Yes	No

(Continued)

10.3389/fmicb.2025.1649750

10.3389/fmicb.2025.1649750

TABLE 1 (Continued)

Overall function as PGPR	Specific functions	Genes	*Caballeronia* sp. RCC-10	*Chitinophaga* sp. RCC-12	*MA-N2* sp. RCC-150	*Paraburkholderia* sp. RCC-158	*Rhizobium* sp. RCC-161.2	*Mucilaginibacter* sp. RCC-168	*Leifsonia* sp. RCC-180	*Terriglobus* sp. RCC-193	*Mesorhizobium* sp. RCC-202	*Variovorax* sp. RCC-210	*Arthrobacter* sp. RCC-34	*Enterobacter* sp. RCC-40	*Luteibacter* sp. RCC-6.2	*Bosea* sp. RCC-152.1	*Bacillus* sp. RCC-6.1
Chemotaxis and motility	Chemotaxis proteins	Chemotaxis protein MotA K02556	Yes	No	No	Yes	Yes	No	Yes	Yes	Yes	Yes	No	Yes	Yes	Yes	Yes
		Chemotaxis protein MotB K02557	Yes	Yes	No	Yes	Yes	Yes	Yes	Yes	Yes	Yes	No	Yes	Yes	Yes	Yes
		Sensor kinase CheA [EC:2.7.13.3]	Yes	No	No	Yes	Yes	No	No	Yes	No	Yes	No	Yes	Yes	Yes	Yes
		Purine-binding chemotaxis protein CheW	Yes	No	No	Yes	Yes	No	No	Yes	No	Yes	No	Yes	Yes	Yes	No
		Chemotaxis protein CheY	Yes	No	No	Yes	Yes	No	No	No	No	Yes	No	Yes	Yes	Yes	No
		Methyl-accepting chemotaxis protein (Mcp) K03406	Yes	No	No	Yes	Yes	No	No	Yes	No	Yes	No	Yes	Yes	Yes	Yes
		chemotaxis protein CheV K03415	Yes	No	No	Yes	No	No	No	No	No	No	No	Yes	Yes	No	Yes
		Protein-glutamate methylesterase/glutaminase [EC:3.1.1.61 3.5.1.44] CheB	Yes	Yes	No	Yes	Yes	Yes	No	Yes	Yes	Yes	No	Yes	Yes	Yes	No
		Chemotaxis protein CheD [EC:3.5.1.44]	Yes	No	No	Yes	Yes	No	No	No	No	Yes	No	No	Yes	Yes	No
		Chemotaxis protein CheC K03410	Yes	No	No	Yes	No	No	No	No	No	No	No	No	No	No	No
		Chemotaxis protein CheZ K03414	Yes	No	No	Yes	No	No	No	No	No	Yes	No	Yes	Yes	No	No
		Chemotaxis protein methyltransferase CheR [EC:2.1.1.80]	Yes	No	No	Yes	Yes	No	No	Yes	No	Yes	No	Yes	Yes	Yes	Yes
	Flagella	Flagellar proteins (fli and flg)	Yes	No	No	Yes	Yes	No	Yes	Yes	Yes	Yes	No	Yes	Yes	Yes	Yes
Mineral phosphate solubilization	Pyrroloquinoline quinone-encoding genes	Quinoprotein glucose dehydrogenase (*gdh*; K00117) [EC:1.1.5.2]	Yes	No	No	Yes	Yes	No	No	No	Yes	No	No	Yes	Yes	No	No
		pqqB (pyrroloquinoline quinone biosynthesis protein B)	Yes	No	No	Yes	Yes	No	No	No	No	No	No	No	No	No	No
		pqqC [EC:1.3.3.11]	Yes	No	No	Yes	Yes	No	No	No	No	No	No	No	No	No	No
		pyrroloquinoline quinone biosynthesis protein D *pqqD*	Yes	No	No	Yes	Yes	No	No	No	No	No	No	No	No	No	No
		pqqE (PqqA peptide cyclase [EC:1.21.98.4]), *pqqF, pqqG, pqqA*	No	No	No	No	No	No	No	No	No	No	No	No	No	No	No
		All three genes *pstABC* (phosphate transport system). K02038, K02036, K02037	Yes	No	Yes	Yes	Yes	No	Yes	Yes	Yes	Yes	Yes	Yes	Yes	Yes	Yes

(Continued)

10.3389/fmicb.2025.1649750

TABLE 1 (Continued)

Overall function as PGPR	Specific functions	Genes	*Caballeronia* sp. RCC-10	*Chitinophaga* sp. RCC-12	*MA-N2* sp. RCC-150	*Paraburkholderia* sp. RCC-158	*Rhizobium* sp. RCC-161.2	*Mucilaginibacter* sp. RCC-168	*Leifsonia* sp. RCC-180	*Terriglobus* sp. RCC-193	*Mesorhizobium* sp. RCC-202	*Variovorax* sp. RCC-210	*Arthrobacter* sp. RCC-34	*Enterobacter* sp. RCC-40	*Luteibacter* sp. RCC-6.2	*Bosea* sp. RCC-152.1	*Bacillus* sp. RCC-6.1
Siderophore to scavenge iron and other essential elements	Siderophore production	*entB (K01252) [EC:3.3.2.1 6.3.2.14] entA (K00216) [EC:1.3.1.28] entD (K02362) [EC:6.3.2.14] entF (K02364) [EC:6.3.2.14 6.2.1.72] entE (K02363)[EC:6.3.2.14 6.2.1.71] entC isochorismate synthase (K02361) [EC:5.4.4.2]*	No	No	No	No	No	No	No	No	No	No	No	Yes	No	No	Yes
	Siderophore transportation	siderophore transport protein TonB	Yes	Yes	No	Yes	Yes	Yes	No	Yes	Yes	Yes	No	Yes	Yes	Yes	No
		siderophore transport protein ExbD	Yes	Yes	No	Yes	No	Yes	No	Yes	Yes	Yes	No	Yes	Yes	Yes	No
		siderophore transport protein ExbB	Yes	Yes	No	Yes	No	Yes	No	Yes	Yes	Yes	No	Yes	Yes	Yes	No
Organic phosphorus mineralization	Phytate mineralization	Alkaline phosphatase D (*phoD*; K01113) [EC:3.1.3.1]	Yes	Yes	No	No	No	Yes	Yes	No	Yes	Yes	No	Yes	No	No	No
		Myo-inositol-hexakisphosphate 4-phosphohydrolase, 4-phytase (EC 3.1.3.26)	No	No	No	No	No	No	No	No	No	No	No	No	Yes	No	No
		Protein tyrosine phosphatase [EC:3.1.3.48]	Yes	Yes	Yes	Yes	No	Yes	Yes	No	Yes	Yes	Yes	Yes	Yes	No	Yes
Exopolysaccharide (EPS) synthesis	Rhizobial exopolysaccharide (EPS)	Exopolysaccharide production protein ExoY (K16566)	No	No	Yes	No	Yes	No	Yes	Yes	Yes	Yes	Yes	No	No	Yes	No
		Succinoglycan biosynthesis protein ExoA (K16557)	No	No	No	No	Yes	No	Yes	No	Yes	No	No	No	No	No	No
		Exopolysaccharide production protein ExoZ (K16568)	Yes	Yes	Yes	Yes	Yes	Yes	Yes	Yes	Yes	Yes	Yes	Yes	Yes	Yes	Yes
		Succinoglycan biosynthesis protein ExoO (K16555), ExoU (K16564), ExoM (K16556), ExoL (K16558)	No	No	No	No	Yes	No	No	No	Yes	No	No	No	No	No	No
		Succinoglycan biosynthesis protein ExoW (K16562), ExoH (K16560), ExoV (K16563)	No	No	No	No	Yes	No	No	No	No	No	No	No	No	No	No
		Succinoglycan biosynthesis protein ExoQ	No	No	No	No	Yes	No	Yes	No	Yes	Yes	No	No	No	No	No
	Vibrio polysachharide	Serine O-acetyltransferase [EC:2.3.1.30], cysE (K00640)	Yes	Yes	Yes	Yes	Yes	Yes	Yes	Yes	Yes	Yes	Yes	Yes	Yes	Yes	Yes

(Continued)

10.3389/fmicb.2025.1649750

TABLE 1 (Continued)

Overall function as PGPR	Specific functions	Genes	*Caballeronia* sp. RCC-10	*Chitinophaga* sp. RCC-12	*MA-N2* sp. RCC-150	*Paraburkholderia* sp. RCC-158	*Rhizobium* sp. RCC-161.2	*Muciliginibacter* sp. RCC-168	*Leifsonia* sp. RCC-180	*Terriglobus* sp. RCC-193	*Mesorhizobium* sp. RCC-202	*Variovorax* sp. RCC-210	*Arthrobacter* sp. RCC-34	*Enterobacter* sp. RCC-40	*Luteibacter* sp. RCC-6.2	*Bosea* sp. RCC-152.1	*Bacillus* sp. RCC-6.1
	Enterobacterial commom antigen pathway	UDP-GlcNAc:undecaprenyl-phosphate [EC:2.7.8.33], WecA (K02851)	No	Yes	Yes	No	No	Yes	Yes	No	No	No	No	Yes	No	No	Yes
		UDP-N-acetyl-D-mannosaminouronate [EC:2.4.1.180], WecG (K02852)	No	No	No	No	No	No	No	No	No	No	No	Yes	No	No	No
		dTDP-N-acetylfucosamine [EC:2.4.1.325], WecF (K12582)	No	No	No	No	No	No	Yes	No	No	No	No	Yes	No	No	No
	Psl polysaccharide	Polysaccharide biosynthesis protein PslA (K20997)	No	No	No	No	Yes	No	No	No	Yes	No	No	No	No	No	No
		Polysaccharide biosynthesis protein PslC (K25205), PslI (K21002)	No	No	No	No	No	No	No	No	No	No	No	No	No	No	No
		Polysaccharide biosynthesis protein PslF (K20999)	No	Yes	No	No	No	Yes	No	No	No	No	No	No	No	No	No
		Polysaccharide biosynthesis protein PslH (K21001)	No	Yes	No	No	Yes	Yes	No	No	Yes	No	No	No	Yes	No	No
	Poly-N-acetyl-glucosamine	Poly-beta-1,6-N-acetyl-D-glucosamine synthase, pgaC, icaA (K11936)	No	Yes	Yes	No	No	Yes	No	Yes	No	Yes	No	Yes	Yes	No	No
		Biofilm PGA synthesis protein PgaD (K11937)	No	No	No	No	No	No	No	No	No	No	No	Yes	Yes	No	No
	Colanic acid synthesis (Extracellular/LPS type)	Colanic acid biosynthesis glycosyltransferase WcaI (K03208)	Yes	Yes	No	Yes	No	Yes	No	Yes	No	Yes	Yes	No	No	No	No
		Colanic acid biosynthesis acetyltransferase WcaF (K03818)	Yes	Yes	No	Yes	No	Yes	No	Yes	No	No	No	Yes	No	No	No
		Colanic acid biosynthesis glycosyltransferase WcaE (K13683)	No	Yes	No	No	No	Yes	No	No	No	No	No	Yes	No	No	No
		Colanic acid biosynthesis glycosyltransferase WcaC (K13684), WcaB (K03819), WcaA (K25875) Undecaprenyl-phosphate glucose phosphotransferase WcaJ (K03606)	No	No	No	No	No	No	No	No	No	No	No	Yes	No	No	No
		Colanic acid biosynthesis glycosyltransferase WcaL (K16703)	No	No	No	No	Yes	No	No	No	No	No	No	Yes	Yes	No	No
		Colanic acid biosynthesis protein WcaK (K16710)	No	No	No	No	No	No	No	No	No	No	No	Yes	Yes	No	No
	EPS regulator genes for *Pseudomonas putida*	surface adhesion protein lapA (K12549)	No	No	No	No	No	No	No	No	No	Yes	No	No	No	No	No
		Cellulose biosynthesis protein BcsQ (PF06564.15)	Yes	No	No	Yes	Yes	No	No	Yes	No	Yes	No	Yes	No	Yes	No
		alginate O-acetyltransferase complex protein AlgI (K19294)	No	Yes	No	No	No	Yes	No	Yes	No	Yes	No	No	Yes	Yes	No

Genes found in the SynCom genomes are highlighted in green, while those that are absent are marked in red.

TABLE 2 Results for the plant growth-promoting (PGP) traits assays in SynCom strains phenotypic characterization.

SynCom isolates	IAA production (ug/ml)	ACC consumed (mM)	Phytate Solubilization (mg/dL)	Siderophore Production	Biofilm formation (OD595)	Gibberlin production (ug/ml)	Acid phosphatase concentration (uM)	Alkaline Phosphatase concentration (uM)
Bosea sp. RCC-152.1		2.25		+	0.282	74.614	616.554	
Luteibacter sp. RCC-6.2		2.03	0.0003		0.337	38.411		
Bacillus sp. RCC-6.1		2.01		+	0.269	101.545		
Enterobacter sp. RCC-40	23.32	1.97		+	0.898	107.726	566.388	375.879
Paraburkholderia sp. RCC-158		1.75		+		65.784	196.436	58.133
Caballeronia sp. RCC-10		1.72			0.359	56.512		
Arthrobacter sp. RCC-34	8.30	1.64			0.736	68.874	15.036	146.804
Variovorax sp. RCC-210		1.61			0.469	32.671		
MA-N2 sp. RCC-150		1.57				52.539		
Terriglobus sp. RCC-193	8.83	1.56	0.0026			65.783		
Chitinophaga sp. RCC-12		1.40		+		2.208	151.573	
Mesorhizobium sp. RCC-202	0.25	1.39			0.259	28.256		
Mucilaginibacter sp. RCC-168	23.32	1.34	0.0043	+	0.316	30.464	47.598	1.124
Leifsonia sp. RCC-180		1.31	0.0065			51.656		
Rhizobium sp. RCC-161.2	3.13	1.17	0.0026	+		58.720		11.394

Results summarizing the phenotypic assays for the plant growth-promoting (PGP) traits in SynCom isolates. For each column/tests darker green represents higher values and lighter color represents smaller values within the column whereas no values represents negative results. 1) IAA production: Amount of IAA produced by the individual isolates when cultured in media containing 0.5mg/mL L-tryptophan and subjected to the Salkowski calorimetric test. 2) ACC deaminase production: Values here indicate the quantity of ACC degraded (in mM) by the individual isolates when cultivated in media supplemented with 3 mM ACC. Higher number represents higher levels of ACC deaminase production. 3) Phytate Solubilization: The values presented here signify the amount of phytate consumed (in mg/dL) by each bacterium during their growth in phytate-specific media containing 0.5 mM Sodium phytate. 4) Siderophore Production: (+) denotes positive siderophore production by the SynCom isolates characterized by the formation of a halo surrounding bacterial cultures upon overlaying with a blue-colored solution after 4 days of growth in a qualitative plate assay. 5) Biofilm formation: Average OD595 values of the wash solution at the end of the biofilm assay of SynCom strains in MS media. The values for OD for the strains that had a significantly higher OD than the negative control (0.216) are listed here. 6) Gibberlin production: Amount of Gibberlin produced by the individual isolates as indicated by the reaction of Gibberlins with Phosphomolybdic acid reagent. 7) Acid phosphatase assay: The numbers represents the average standardized concentration of p-nitrophenol (uM) in Acetate Buffer (pH = 5) representing acid phosphatase activity in the isolates. 8) Alkaline phosphatase assay: The numbers represents the average standardized concentration p-nitrophenol (uM) in Boric Buffer (pH = 9) representing alkaline phosphatase activity in the isolates.

10.3389/fmicb.2025.1649750

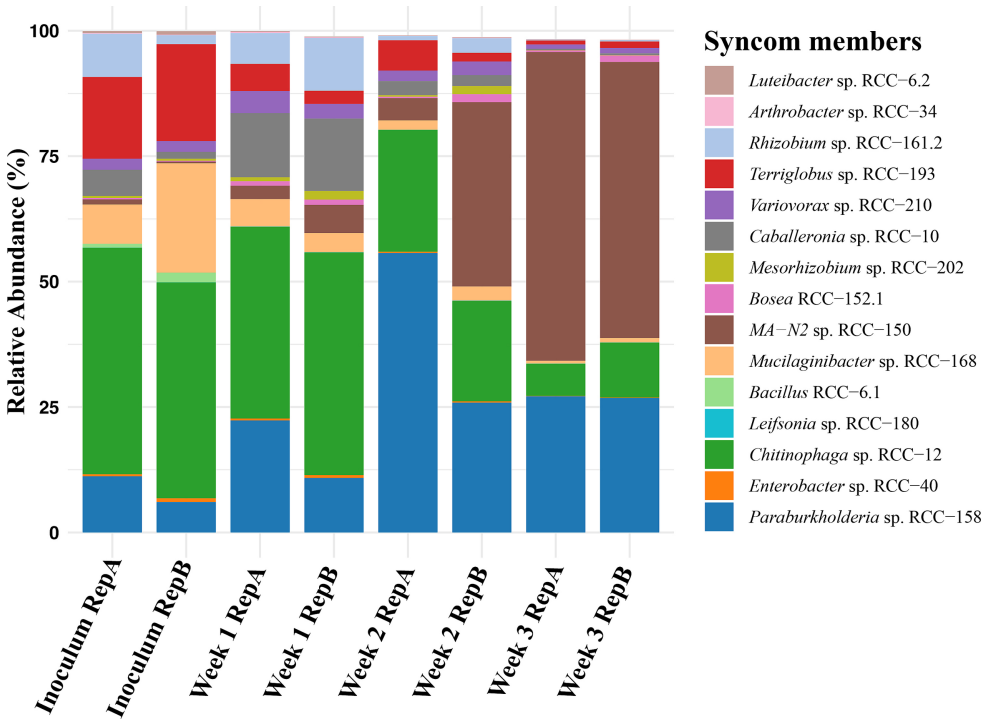

FIGURE 3
Stability of Syncom members: Changes in the microbial community over 3 weeks when the 15-member SynCom is cultured in 0.2X MS media and transferred weekly. The initial bar on the x-axis reflects the relative abundance of 15 SynCom members in the Inoculum, followed by pairs of bars representing duplicates for samples taken at the end of Weeks 1, 2, and 3. The Y-axis shows the relative abundances of each SynCom strain which is represented by a different color as shown in the legend.

When examining SynCom persistence under the above stress conditions, we observed that all strains were persistent throughout drought, rewatered drought, and salinity stress after 3 weeks (Figures 4B, 5B). However, significant differences in relative abundance of the individual strains were observed. Under drought, *Paraburkholderia* sp. RCC-158 (lfc = 1.29), *Rhizobium* sp. RCC-161.2 (lfc = 1.91), *Mesorhizobium* sp. RCC-202 (lfc = 1.82), *Terriglobus* sp. RCC-193 (lfc = 3.09), and *Chitinophaga* sp. RCC-12 (lfc = 1.96) showed significant ($p < 0.05$, two-sided Chi-square test) decreases in log fold change (lfc) relative abundance (Figure 4C) compared to the no-stress control. In rewatered drought conditions, *Terriglobus* sp. RCC-193 (lfc = 1.74) showed a significant decrease, while *MA-N2* sp. RCC-150 (lfc = 1.4), *Leifsonia* sp. RCC-180 (lfc = 1.04), and *Caballeronia* sp. RCC-10 (lfc = 1.09) significantly increased (Figure 4D) relative to controls. No significant change in SynCom relative abundance was observed under salinity stress (Figure 5C).

SynCom strains exhibit distinct spatial localization on the root

Previous studies have highlighted that plants secrete specific compounds as root exudates to recruit select microbes, especially under stressful conditions (Vives-Peris et al., 2020). Given that exudation might vary between root tips and base (Dragišić Maksimović et al., 2021), we investigated the recruitment and spatial localization of SynCom strains on different parts of the root in the experiments above (drought and salinity stress). The SynCom was applied to the seedling's growing root base for both these tests, and at the completion of the experiments, we analyzed the community at both the root tip and root base using 16S rRNA-based amplicon sequencing. Distinct colonization patterns emerged for certain strains. Under no stress, strains such as *MA-N2* sp. RCC-150, *Mucilaginibacter* sp. RCC-168, Var*iovorax* sp. RCC-210, and *Arthrobacter* sp. RCC-34 were significantly enriched (t-test) at the root base compared to their abundance in the inoculum and root tips (Figure 6, control sets). Under drought stress, however, *Luteibacter* sp. RCC-6.2 and *Arthrobacter* sp. RCC-34 showed increased abundance at the base, while *MA-N2* sp. RCC-150 was significantly enriched at the root tip. In rewatered drought conditions, *MA-N2* sp. RCC-150 and *Leifsonia* sp. RCC-180 were more abundant at the root tip. During salinity stress, *MA-N2* sp. RCC-150 was the only strain found to have significantly increased abundance at the root tip. Overall, *MA-N2* sp. RCC-150 displayed a notable preference for the root tip, especially under salt and drought stress conditions.

Discussion

We developed a framework to integrate both culture-dependent and culture-independent approaches toward creating a stable SynCom that interacts positively with the host plant and confers beneficial traits during adverse environmental conditions. To do this, several strains were isolated from a *Brachypodium* rhizosphere enriched community, and selection of a subset was designed informed by 16S rDNA amplicon sequencing of enriched communities, and network analysis, which revealed both positive and negative microbial interactions within the enriched community (Chen et al., 2024; Figure 1). These

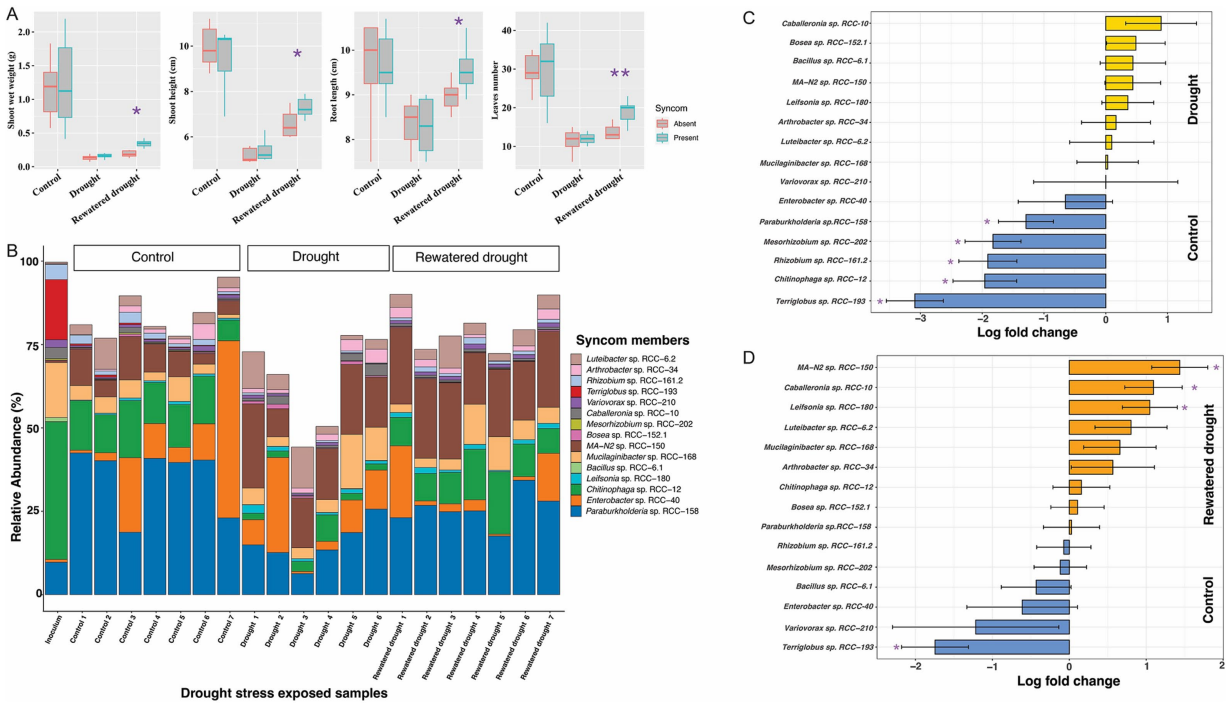

FIGURE 4
Figures depicting the plant phenotypic traits and microbial 16S rRNA gene abundances profile from the SynCom drought stress experiment. The experiment comprised three sets: the Control set, Drought set, and Rewatered Drought set. **(A)** Plant phenotype results: Comparisons for the shoot weight, shoot height, root length, and leaves numbers in *Brachypodium*, with and without SynCom members, during a 3-week exposure to drought stress. Each experimental category included seven *Brachypodium* plants. Significant values determined by t-tests are indicated by purple asterisks positioned above the corresponding bars. **(B)** 16S rRNA gene abundances profiles: In the barplot, each bar represents a replicate (shown in x-axis) in the corresponding experimental set as indicated above the bars. Y-axis shows the relative abundances values for each SynCom isolates represented by different color in legend, while all other bacterial groups are combined into the "Others" group, depicted in white on the plot. It is important to note that certain DNA samples in the experimental sets, i.e., rewatered drought encountered sequencing issues, leading to a reduced sample size of 5. **(C)** The natural log fold changes (lfc) for SynCom strains in stress conditions, as measured by "ANCOMBC" with drought (yellow) and **(D)** rewatered drought (orange), when compared to the SynCom-amended control plants (blue). On y-axis, negative values indicate that taxa are more abundant in control conditions, while positive values show greater abundance in drought or rewatered drought conditions. Bars indicate changes in the natural log fold, and error bars represent standard errors. Asterisks indicate significant changes in the natural log fold after the Benjamini-Hochberg adjustment of the false discovery rate ($p < 0.05$).

interactions informed the final selection of microbial members of the SynCom, ensuring ecological relevance and functional integrity (Toju et al., 2020). At the end of our data-driven SynCom assembly, the final 15 strains included representation from five different phyla (Figure 2). Notably, *Mesorhizobium* sp. RCC-202, a keystone species identified in the network analysis (Figure 1), was included for its critical role in shaping microbial community structure and dynamics that likely contributes to the SynCom's robustness (Agler et al., 2016). We were also successful in including *Terriglobus* (*Terriglobus* sp. RCC-193), a genus within Acidobacteria known for its ecological significance in soil and its challenging cultivation, highlighting our effort to incorporate underexplored yet essential microbial taxa (Eichorst et al., 2007; Kalam et al., 2022). A persistent challenge in SynCom development for enhancing plant productivity is identifying which specific microbial members actually contribute to community stability and functional outcomes (Pradhan et al., 2022; Sun et al., 2025; O'Banion et al., 2020). Here, we were successful in assembling a Syncom with the keystone species based on network interaction (Figure 1) and fairly persistent microbial culture propagated *in vitro* (Figure 3). In subsequent experiments, we show that all SynCom members demonstrated persistence in the *Brachypodium* rhizosphere over a period of 3 weeks, even under stress conditions (Figures 4, 5). Notably, their improved persistence and more balanced relative abundance *in planta* compared to *in vitro,* suggest positive interactions with the host plant, an often-overlooked criterion in previous SynCom studies (Sanchez-Gorostiaga et al., 2018; Toju et al., 2020; Werner and Kiers, 2015; Kabir et al., 2024). Additionally, the sustained presence of Gram-positive bacteria, in particular, is noteworthy due to their role and potential for use as microbial amendments in agricultural applications for enhancing host plant resilience during environmental stress (Schimel et al., 2007; Qi et al., 2022).

We examined specific colonization of the SynCom members along the root of *Brachypodium distachyon* (Figure 6). It is generally accepted that the spatial distribution of microbes along the root surface is in direct response to differential root exudation and gradients thereof (Wei et al., 2021; Acharya et al., 2023b). We observed a strong preference for colonization at the root tip under stress conditions (Figure 6), which demonstrates that the microbes migrated to the root tip with the growing root despite being inoculated initially to the root base. This was particularly evident for Gram-positive strains such as *MA-N2* sp. RCC-150, *Leifsonia* sp. RCC-180, and *Bacillus* sp. RCC-6.1 (Figure 6). Since the root tip is the most actively growing part of the root, this result indicates that when growing under stress, the plant is actively seeking to recruit specific microbes that help with stress alleviation. It is known that *Brachypodium* increases production of levels of metabolites like proline and soluble sugars in

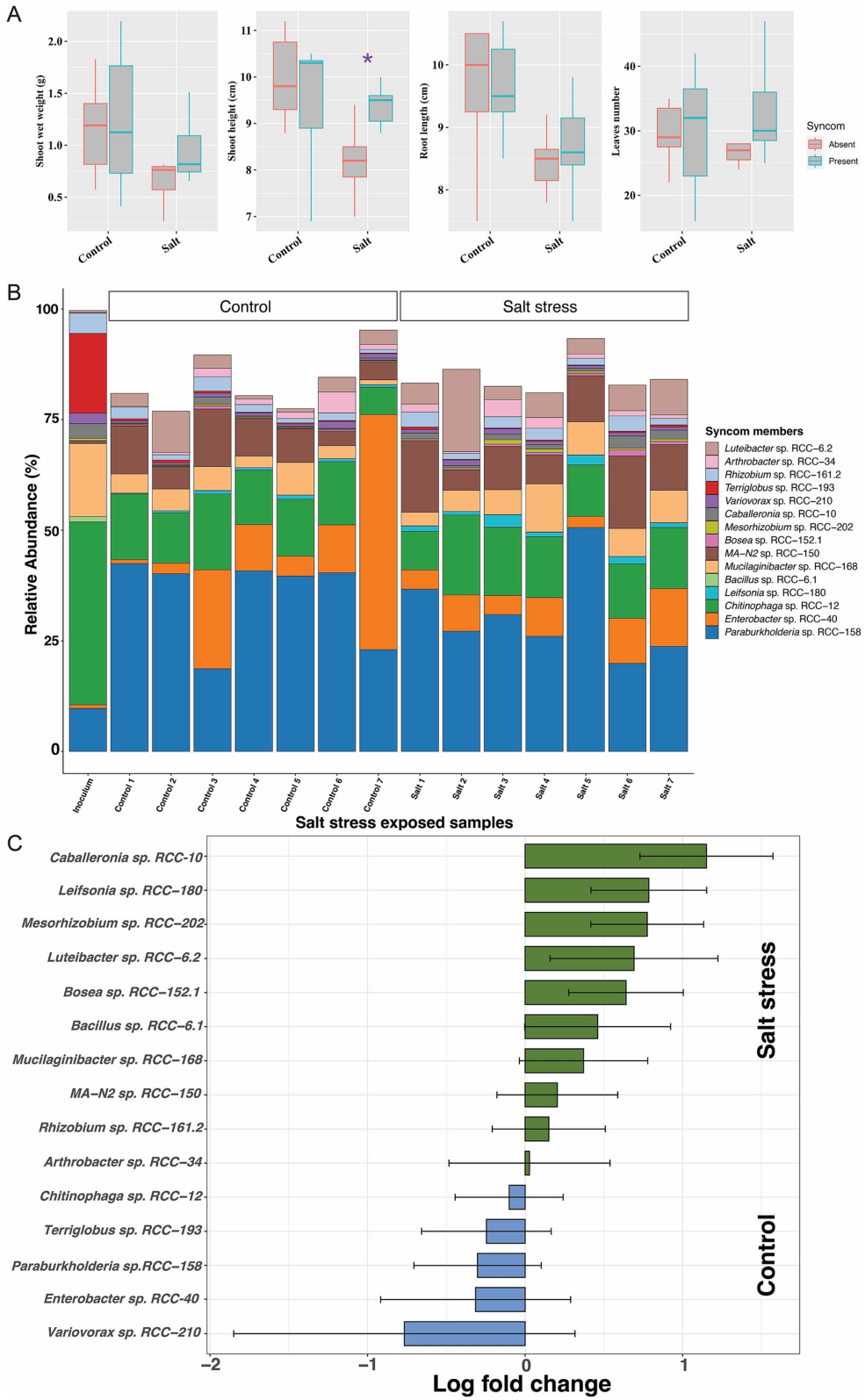

FIGURE 5
Figures depicting the plant phenotypic traits microbial 16S rRNA gene abundances profile from the SynCom salt stress experiment. The experiment comprised two sets, i.e., the Control set and the Salt stress. **(A)** Plant phenotype result: Comparisons for the shoot weight, shoot height, root length and leaves numbers in *Brachypodium*, with and without SynCom members, during a 3-week exposure to salt stress. Each experimental category included seven *Brachypodium* plants. Significant values determined by t-tests are indicated by purple asterisks positioned above the corresponding bars. **(B)** 16S rRNA gene abundance profiles: In the barplot, each bar represents a replicate (shown in x-axis) in the corresponding experimental set as

(Continued)

FIGURE 5 (Continued)
indicated above the bars. Y-axis shows the relative abundances values for each Syncom isolate represented by different color in the legend, while all other bacterial groups are combined into the "Others" group, depicted in white on the plot. **(C)** The natural log fold changes (lfc) for SynCom strains in stress conditions, as measured by "ANCOMBC" with salt stress (green) when compared to the SynCom-amended control plants (blue). On y-axis, negative values indicate that taxa are more abundant in control conditions, while positive values show greater abundance in salt conditions. Bars indicate changes in the natural log fold, and error bars represent standard errors. None of the SynCom members was found to have significant changes in natural log fold after the Benjamini-Hochberg adjustment of false discovery rate ($p < 0.05$).

drought-tolerant varieties (Shi et al., 2015). These compounds can serve as chemoattractant and carbon sources for Gram-positive bacteria (Gagné-Bourque et al., 2015; Sharma et al., 2020). Therefore it is reasonable to assume that Gram-positive bacteria, such as Actinobacteria and Bacilli, produce metabolites that assist in drought stress tolerance are attracted to the root tip through these root exudate compounds (Ek-Ramos et al., 2019; Grover et al., 2016). Our carbon-utilization phenotypic assays (Supplementary Figure S1) revealed that the Gram-positive taxa—*MA-N2* sp. RCC-150, *Leifsonia* sp. RCC-180, and *Arthrobacter* sp. RCC-34—each metabolized large subsets of metabolites that significantly enriched during the drought stress (e.g., proline, malate, sucrose). Notably, *MA-N2* sp. RCC-150 and *Arthrobacter* sp. RCC-34 were among only three isolates able to utilize malate, a key drought-linked carbon source that increased significantly in both roots and leaves for *Brachypodium* (Ahkami et al., 2019). This in vitro preference for osmoprotectants and sugars parallels their in planta enrichment at the growing root tip, underscoring their role in exploiting exudates under stress. Specifically, *MA-N2* sp. RCC-150 showed increased overall abundance during rewatered drought conditions (Figure 4) and was enriched at the root tips during both drought and rewatered drought (Figure 6). The root tip is often considered to be the part of the root of active root exudation. Therefore this enrichment is likely due to multiple factors, including the strain's ability to respond to specific root exudate metabolites (Supplementary Figure S1) or, ability to return to the plant trehalose and various exopolysaccharides that potentially benefit the plant during drought stress (Table 1).

When we compared growth of *Brachypodium* in SynCom-amended and unamended treatments under different stress conditions, we found that the SynCom exhibited substantially higher functional redundancy under drought and rewatered drought conditions compared to no-stress conditions (Supplementary Figure S5). This suggests that bacterial strains enriched during stress encode overlapping PGP traits (Table 1), with functional redundancy likely acting as a buffer to maintain critical microbial functions despite shifts in community composition. These findings align with evidence that plants under stress modulate their rhizosphere microbiomes based on shared PGP functions rather than recruiting specific taxa (Louca et al., 2018; Zia et al., 2021). Notably, while significant changes in SynCom composition occurred during both drought and rewatered drought treatments, measurable enhancements in plant phenotypes, such as above- and below-ground biomass, and root and shoot heights, were observed only in rewatered drought treatments (Figure 4A). These observations align with emerging research suggesting microbial effects on plant recovery post-stress can be more pronounced than during the stress itself (Bandopadhyay et al., 2024). It is known that many bacteria enter dormant or low-metabolism states to conserve energy during drought stress (de Vries et al., 2020). Upon rehydration, microbial communities can rapidly rebound, with increased metabolic activity from the host plants including flush of root exudates (Canarini et al., 2019), colonization, and production of plant growth-promoting compounds such as auxins, gibberellins, and ACC deaminase (Rolli et al., 2015; Ngumbi and Kloepper, 2016). Furthermore, microbial consortia may "prime" plants during drought for enhanced resilience, with effects becoming measurable only once stress is relieved and growth resumes (Santos-Medellín et al., 2017).

Recognizing that microbial effects on plants are often more pronounced during post-stress recovery than during the stress itself, the notable benefits of SynCom to host plants during the rewatered drought conditions can be attributed to several factors. First, the isolates with significantly increased relative abundance under rewatered drought (e.g., *MA-N2* sp. RCC-150, *Caballeronia* sp. RCC-10, and *Leifsonia* sp. RCC-180; Figure 4D), belong to genera known to alleviate drought stress in plants (Nordstedt et al., 2021; Platamone et al., 2023), and their genomes encode genes for producing osmoprotectant compounds (Supplementary Table S2) and exopolysaccharide production protein (Table 1). Second, several other SynCom strains harbor genes critical for managing drought and salinity stresses, including genes for trehalose biosynthesis (Kosar et al., 2018; Sharma et al., 2020; Hassan et al., 2023), sodium and potassium transporters (Ahmad et al., 2022; Gunde-Cimerman et al., 2018), and ACC deaminase (Orozco-Mosqueda et al., 2020; Table 1). Third, we observed enhanced positive interactions among SynCom strains, particularly during rewatered drought (22 positive and 7 negative, Supplementary Figure S6). These positive microbial interactions likely promoted overall microbial community functionality and benefited the host plant (Layeghifard et al., 2017; Martins et al., 2023). Our findings overall demonstrate that SynCom persists under drought conditions and supports more effective plant recovery post-drought, emphasizing their potential role for applications in enhancing crop resilience and productivity amid climate variability. While we can postulate that certain genes and traits of the SynCom strains play a role in alleviating drought, future experiments exploring gene-expression and metabolite production are needed to confirm.

To summarize, in this study, we developed a 15-member SynCom from the rhizobiome of *Brachypodium distachyon* using an integrative framework that combined culture-dependent and culture-independent methods, guided by network analysis to ensure ecological relevance and functional integrity. The SynCom demonstrated persistence, stability when grown with plants, and conferred resilience under stress conditions, aiding plant recovery during rewatering after drought. These findings highlight the SynCom's potential for agricultural applications in improving crop resilience and supporting recovery after drought or salinity stress. Future research exploring SynCom influence on plant gene expression and vice versa under drought and salt stress will further help optimize the use and application of this SynCom in diverse

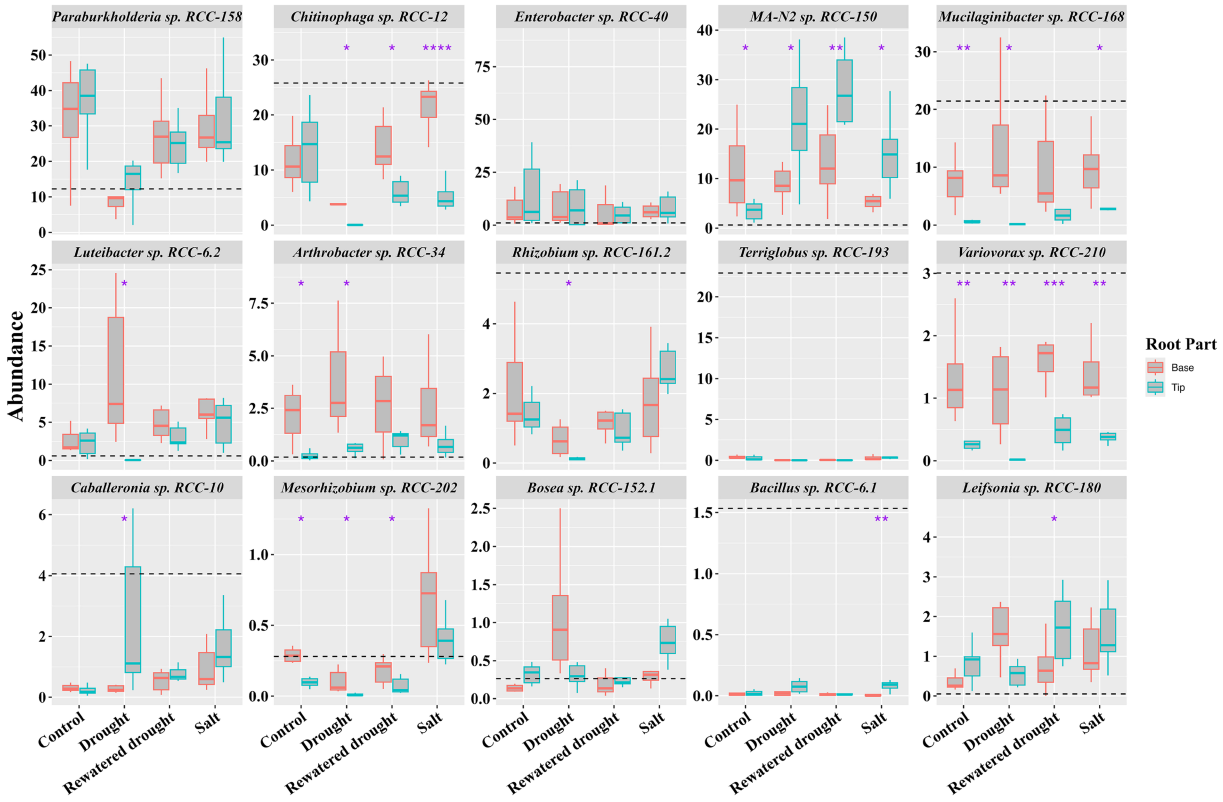

FIGURE 6
Spatial localization of SynCom strains in the Brachypodium root system: Boxplots show the 16S rRNA gene abundances for the SynCom isolates across the root tip and base in SynCom-amended plants under control and drought and salt stress conditions (as indicated on the x-axis) after 21 days. The y-axis displays the relative percentage abundances of the SynCom members indicated atop each boxplot panel. Significant differences determined by t-tests between the root parts (tip and base) within each condition are marked with an asterisk above and between the respective bars. The black horizontal dashed line indicates the percentage of strain abundance in the inoculum.

agricultural systems, ensuring scalability and efficacy in mitigating climate-related challenges.

Data availability statement

The datasets presented in this study can be found in online repositories. The names of the repository/repositories and accession number(s) can be found at: https://www.ncbi.nlm.nih.gov/genbank/, PRJNA1127609. The KBase narrative containing the genome assemblies and annotation tools run on the assemblies are also publicly available at narrative.kbase.us/narrative/135275.

Author contributions

AY: Visualization, Validation, Data curation, Formal analysis, Methodology, Writing – review & editing, Writing – original draft, Conceptualization, Investigation. MC: Investigation, Writing – review & editing, Conceptualization, Writing – original draft, Validation, Visualization, Methodology, Data curation, Formal analysis. SA: Writing – original draft, Methodology, Conceptualization, Investigation, Data curation, Writing – review & editing. GK: Methodology, Data curation, Investigation, Formal analysis, Writing – review & editing. YY: Formal analysis, Data curation, Writing – review & editing, Methodology, Investigation. TZ: Writing – review & editing, Data curation, Formal analysis, Investigation. ET: Writing – review & editing, Investigation, Data curation. RC: Funding acquisition, Supervision, Writing – original draft, Resources, Writing – review & editing, Investigation, Conceptualization, Project administration.

Funding

The author(s) declare that financial support was received for the research and/or publication of this article. This research work was funded through Microbial Community Analysis & Functional Evaluation in Soils (m-CAFEs), a Science Focus Area led by Lawrence Berkeley National Laboratory funded by the U. S. Department of Energy, Office of Science, Office of Biological Environmental Research under contract number DE-AC02-05CH11231.

Conflict of interest

The authors declare that the research was conducted in the absence of any commercial or financial relationships that could be construed as a potential conflict of interest.

The author(s) declared that they were an editorial board member of Frontiers, at the time of submission. This had no impact on the peer review process and the final decision.

Generative AI statement

The author(s) declare that no Gen AI was used in the creation of this manuscript.

Publisher's note

All claims expressed in this article are solely those of the authors and do not necessarily represent those of their affiliated organizations, or those of the publisher, the editors and the reviewers. Any product that may be evaluated in this article, or claim that may be made by its manufacturer, is not guaranteed or endorsed by the publisher.

Supplementary material

The Supplementary material for this article can be found online at: https://www.frontiersin.org/articles/10.3389/fmicb.2025.1649750/full#supplementary-material

References

Acharya, S. M., Enalls, B. C., Walian, P. J., Van Houghton, B. D., Rosenblum, J. S., Cath, T. Y., et al. (2023a). *Iodidimonas*, a bacterium unable to degrade hydrocarbons, thrives in a bioreactor treating oil and gas produced water. *BioRxiv*. doi: 10.1101/2023.03.02.530844

Acharya, S. M., Yee, M. O., Diamond, S., Andeer, P. F., Baig, N. F., Aladesanmi, O. T., et al. (2023b). Fine scale sampling reveals early differentiation of rhizosphere microbiome from bulk soil in young Brachypodium plant roots. *ISME Commun.* 3:54. doi: 10.1038/s43705-023-00265-1

Agler, M. T., Ruhe, J., Kroll, S., Morhenn, C., Kim, S.-T., Weigel, D., et al. (2016). Microbial hub taxa link host and abiotic factors to plant microbiome variation. *PLoS Biol.* 14:e1002352. doi: 10.1371/journal.pbio.1002352

Ahkami, A. H., Wang, W., Wietsma, T. W., Winkler, T., Lange, I., Jansson, C., et al. (2019). Metabolic shifts associated with drought-induced senescence in Brachypodium. *Plant Sci.* 289:110278. doi: 10.1016/j.plantsci.2019.110278

Ahmad, H. M., Fiaz, S., Hafeez, S., Zahra, S., Shah, A. N., Gul, B., et al. (2022). Plant growth-promoting Rhizobacteria eliminate the effect of drought stress in plants: a review. *Front. Plant Sci.* 13:875774. doi: 10.3389/fpls.2022.875774

Allison, S. D., Gartner, T. B., Holland, K., Weintraub, M., and Sinsabaugh, R. L. (2007). Soil enzymes: linking proteomics and ecological processes. *Manual of environmental microbiology* 704–711. doi: 10.1128/9781555815882.ch58

Arkin, A. P., Cottingham, R. W., Henry, C. S., Harris, N. L., Stevens, R. L., Maslov, S., et al. (2018). KBase: the United States Department of Energy Systems Biology Knowledgebase. *Nat. Biotechnol.* 36, 566–569. doi: 10.1038/nbt.4163

Atta, K., Mondal, S., Gorai, S., Singh, A. P., Kumari, A., Ghosh, T., et al. (2023). Impacts of salinity stress on crop plants: improving salt tolerance through genetic and molecular dissection. *Front. Plant Sci.* 14:1241736. doi: 10.3389/fpls.2023.1241736

Bandopadhyay, S., Li, X., Bowsher, A. W., Last, R. L., and Shade, A. (2024). Disentangling plant- and environment-mediated drivers of active rhizosphere bacterial community dynamics during short-term drought. *Nat. Commun.* 15:6347. doi: 10.1038/s41467-024-50463-1

Berendsen, R. L., Vismans, G., Yu, K., Song, Y., de Jonge, R., Burgman, W. P., et al. (2018). Disease-induced assemblage of a plant-beneficial bacterial consortium. *ISME J.* 12, 1496–1507. doi: 10.1038/s41396-018-0093-1

Bergelson, J., Mittelstrass, J., and Horton, M. W. (2019). Characterizing both bacteria and fungi improves understanding of the Arabidopsis root microbiome. *Sci. Rep.* 9:24. doi: 10.1038/s41598-018-37208-z

Bhattacharyya, P. N., and Jha, D. K. (2012). Plant growth-promoting rhizobacteria (PGPR): emergence in agriculture. *World J. Microbiol. Biotechnol.* 28, 1327–1350. doi: 10.1007/s11274-011-0979-9

Bolger, A. M., Lohse, M., and Usadel, B. (2014). Trimmomatic: a flexible trimmer for Illumina sequence data. *Bioinformatics* 30, 2114–2120. doi: 10.1093/bioinformatics/btu170

Bolyen, E., Rideout, J. R., Dillon, M. R., Bokulich, N. A., Abnet, C. C., Al-Ghalith, G. A., et al. (2019). Reproducible, interactive, scalable and extensible microbiome data science using QIIME 2. *Nat. Biotechnol.* 37, 852–857. doi: 10.1038/s41587-019-0209-9

Bruto, M., Prigent-Combaret, C., Muller, D., and Moënne-Loccoz, Y. (2014). Analysis of genes contributing to plant-beneficial functions in plant growth-promoting Rhizobacteria and related Proteobacteria. *Sci. Rep.* 4:6261. doi: 10.1038/srep06261

Bulgarelli, D., Garrido-Oter, R., Münch, P. C., Weiman, A., Dröge, J., Pan, Y., et al. (2015). Structure and function of the bacterial root microbiota in wild and domesticated barley. *Cell Host Microbe* 17, 392–403. doi: 10.1016/j.chom.2015.01.011

Canarini, A., Kaiser, C., Merchant, A., Richter, A., and Wanek, W. (2019). Root exudation of primary metabolites: mechanisms and their roles in plant responses to environmental stimuli. *Front. Plant Sci.* 10:157. doi: 10.3389/fpls.2019.00157

Chakraborty, R., Woo, H., Dehal, P., Walker, R., Zemla, M., Auer, M., et al. (2017). Complete genome sequence of *Pseudomonas stutzeri* strain RCH2 isolated from a hexavalent chromium [Cr(VI)] contaminated site. *Stand. Genomic Sci.* 12:23. doi: 10.1186/s40793-017-0233-7

Chaumeil, P.-A., Mussig, A. J., Hugenholtz, P., and Parks, D. H. (2022). GTDB-Tk v2: memory friendly classification with the genome taxonomy database. *Bioinformatics* 38, 5315–5316. doi: 10.1093/bioinformatics/btac672

Chen, M., Acharya, S. M., Yee, M. O., Cabugao, K. G. M., and Chakraborty, R. (2024). Developing stable, simplified, functional consortia from Brachypodium rhizosphere for microbial application in sustainable agriculture. *Front. Microbiol.* 15:1401794. doi: 10.3389/fmicb.2024.1401794

Chodkowski, J. L., and Shade, A. (2017). A synthetic community system for probing microbial interactions driven by exometabolites. *mSystems* 2:375. doi: 10.1128/mSystems.00129-17

Darling, P., Chan, M., Cox, A. D., and Sokol, P. A. (1998). Siderophore production by cystic fibrosis isolates of *Burkholderia cepacia*. *Infect. Immun.* 66, 874–877.

de Bello, F., Carmona, C. P., Dias, A. T. C., Götzenberger, L., Moretti, M., and Berg, M. P. (2021). Handbook of trait-based ecology: From theory to R tools. *1st* Edn. Cambridge, UK: Cambridge University Press.

de Souza, R. S. C., Armanhi, J. S. L., and Arruda, P. (2020). From microbiome to traits: designing synthetic microbial communities for improved crop resiliency. *Front. Plant Sci.* 11:1179. doi: 10.3389/fpls.2020.01179

de Vries, F. T., Griffiths, R. I., Knight, C. G., Nicolitch, O., and Williams, A. (2020). Harnessing rhizosphere microbiomes for drought-resilient crop production. *Science* 368, 270–274. doi: 10.1126/science.aaz5192

Debastiani, V. J., and Pillar, V. D. (2012). SYNCSA--R tool for analysis of metacommunities based on functional traits and phylogeny of the community components. *Bioinformatics* 28, 2067–2068. doi: 10.1093/bioinformatics/bts325

Diwan, D., Rashid, M. M., and Vaishnav, A. (2022). Current understanding of plant-microbe interaction through the lenses of multi-omics approaches and their benefits in sustainable agriculture. *Microbiol. Res.* 265:127180. doi: 10.1016/j.micres.2022.127180

Dodd, I. C., Zinovkina, N. Y., Safronova, V. I., and Belimov, A. A. (2010). Rhizobacterial mediation of plant hormone status. *Ann. Appl. Biol.* 157, 361–379. doi: 10.1111/j.1744-7348.2010.00439.x

Dragišić Maksimović, J., Mojović, M., Vučinić, Ž., and Maksimović, V. (2021). Spatial distribution of apoplastic antioxidative constituents in maize root. *Physiol. Plant.* 173, 818–828. doi: 10.1111/ppl.13476

Eichmann, R., Richards, L., and Schäfer, P. (2021). Hormones as go-betweens in plant microbiome assembly. *Plant J.* 105, 518–541. doi: 10.1111/tpj.15135

Eichorst, S. A., Breznak, J. A., and Schmidt, T. M. (2007). Isolation and characterization of soil bacteria that define Terriglobus gen. Nov., in the phylum Acidobacteria. *Appl. Environ. Microbiol.* 73, 2708–2717. doi: 10.1128/AEM.02140-06

Ek-Ramos, M. J., Gomez-Flores, R., Orozco-Flores, A. A., Rodríguez-Padilla, C., González-Ochoa, G., and Tamez-Guerra, P. (2019). Bioactive products from plant-Endophytic gram-positive Bacteria. *Front. Microbiol.* 10:463. doi: 10.3389/fmicb.2019.00463

Finkel, O. M., Castrillo, G., Herrera Paredes, S., Salas González, I., and Dangl, J. L. (2017). Understanding and exploiting plant beneficial microbes. *Curr. Opin. Plant Biol.* 38, 155–163. doi: 10.1016/j.pbi.2017.04.018

Fisher, L. H. C., Han, J., Corke, F. M. K., Akinyemi, A., Didion, T., Nielsen, K. K., et al. (2016). Linking dynamic phenotyping with metabolite analysis to study natural variation in drought responses of *Brachypodium distachyon*. *Front. Plant Sci.* 7:1751. doi: 10.3389/fpls.2016.01751

Flores-Duarte, N. J., Navarro-Torre, S., Mateos-Naranjo, E., Redondo-Gómez, S., Pajuelo, E., and Rodríguez-Llorente, I. D. (2023). Nodule synthetic bacterial community as legume biofertilizer under abiotic stress in estuarine soils. *Plants* 12:2083. doi: 10.3390/plants12112083

Gagné-Bourque, F., Mayer, B. F., Charron, J.-B., Vali, H., Bertrand, A., and Jabaji, S. (2015). Accelerated growth rate and increased drought stress resilience of the model

grass *Brachypodium distachyon* colonized by *Bacillus subtilis* B26. *PLoS One* 10:e0130456. doi: 10.1371/journal.pone.0130456

Gilbert, S., Xu, J., Acosta, K., Poulev, A., Lebeis, S., and Lam, E. (2018). Bacterial production of indole related compounds reveals their role in association between duckweeds and endophytes. *Front. Chem.* 6:265. doi: 10.3389/fchem.2018.00265

Gkarmiri, K., Mahmood, S., Ekblad, A., Alström, S., Högberg, N., and Finlay, R. (2017). Identifying the active microbiome associated with roots and rhizosphere soil of oilseed rape. *Applied and Environmental Microbiology* 83, e01938–e01917. doi: 10.1128/AEM.01938-17

Gombos, M., Hapek, N., Kozma-Bognár, L., Grezal, G., Zombori, Z., Kiss, E., et al. (2023). Limited water stress modulates expression of circadian clock genes in *Brachypodium distachyon* roots. *Sci. Rep.* 13:1241. doi: 10.1038/s41598-022-27287-4

Gonçalves, O. S., Creevey, C. J., and Santana, M. F. (2023). Designing a synthetic microbial community through genome metabolic modeling to enhance plant-microbe interaction. *Environ. Microbiome* 18:81. doi: 10.1186/s40793-023-00536-3

Graham, H. D., and Henderson, J. H. (1961). Reaction of gibberellic acid & gibberellins with Folin-Wu phosphomolybdic acid reagent & its use for quantitative assay. *Plant Physiol.* 36, 405–408.

Grover, M., Bodhankar, S., Maheswari, M., and Srinivasarao, C. (2016). "Actinomycetes as mitigators of climate change and abiotic stress" in Plant growth promoting actinobacteria. eds. G. Subramaniam, S. Arumugam and V. Rajendran (Singapore: Springer Singapore), 203–212.

Gunde-Cimerman, N., Plemenitaš, A., and Oren, A. (2018). Strategies of adaptation of microorganisms of the three domains of life to high salt concentrations. *FEMS Microbiol. Rev.* 42, 353–375. doi: 10.1093/femsre/fuy009

Gupta, R., Anand, G., Gaur, R., and Yadav, D. (2021). Plant-microbiome interactions for sustainable agriculture: a review. *Physiol. Mol. Biol. Plants* 27, 165–179. doi: 10.1007/s12298-021-00927-1

Gupta, A., Gopal, M., Thomas, G. V., Manikandan, V., Gajewski, J., Thomas, G., et al. (2014). Whole genome sequencing and analysis of plant growth promoting bacteria isolated from the rhizosphere of plantation crops coconut, cocoa and arecanut. *PLoS One* 9:e104259. doi: 10.1371/journal.pone.0104259

Gurevich, A., Saveliev, V., Vyahhi, N., and Tesler, G. (2013). QUAST: quality assessment tool for genome assemblies. *Bioinformatics* 29, 1072–1075. doi: 10.1093/bioinformatics/btt086

Gutleben, J., Chaib De Mares, M., van Elsas, J. D., Smidt, H., Overmann, J., and Sipkema, D. (2018). The multi-omics promise in context: from sequence to microbial isolate. *Crit. Rev. Microbiol.* 44, 212–229. doi: 10.1080/1040841X.2017.1332003

Haney, E. F., Trimble, M. J., and Hancock, R. E. W. (2021). Microtiter plate assays to assess antibiofilm activity against bacteria. *Nat. Protoc.* 16, 2615–2632. doi: 10.1038/s41596-021-00515-3

Hao, S., Wang, Y., Yan, Y., Liu, Y., Wang, J., and Chen, S. (2021). A review on plant responses to salt stress and their mechanisms of salt resistance. *Horticulturae* 7:132. doi: 10.3390/horticulturae7060132

Hassan, M. U., Nawaz, M., Shah, A. N., Raza, A., Barbanti, L., Skalicky, M., et al. (2023). Trehalose: a key player in plant growth regulation and tolerance to abiotic stresses. *J. Plant Growth Regul.* 42, 4935–4957. doi: 10.1007/s00344-022-10851-7

Hosseinkhani, B., and Hosseinkhani, G. (2009). Analysis of phytase producing bacteria (Pseudomonas sp.) from poultry faeces and optimization of this enzyme production. *African Journal of Biotechnology* 8, 4229–4232.

Ingram, P. A., Zhu, J., Shariff, A., Davis, I. W., Benfey, P. N., and Elich, T. (2012). High-throughput imaging and analysis of root system architecture in *Brachypodium distachyon* under differential nutrient availability. *Philos. Trans. R. Soc. Lond. Ser. B Biol. Sci.* 367, 1559–1569. doi: 10.1098/rstb.2011.0241

Kabir, A. H., Baki, M. Z. I., Ahmed, B., and Mostofa, M. G. (2024). Current, faltering, and future strategies for advancing microbiome-assisted sustainable agriculture and environmental resilience. *New Crops.* 1:100013. doi: 10.1016/j.ncrops.2024.100013

Kalam, S., Basu, A., and Podile, A. R. (2022). Difficult-to-culture bacteria in the rhizosphere: the underexplored signature microbial groups. *Pedosphere* 32, 75–89. doi: 10.1016/S1002-0160(21)60062-0

Kanehisa, M., and Sato, Y. (2020). KEGG mapper for inferring cellular functions from protein sequences. *Protein Sci.* 29, 28–35. doi: 10.1002/pro.3711

Kanehisa, M., Sato, Y., and Morishima, K. (2016). Blastkoala and ghostkoala: KEGG tools for functional characterization of genome and metagenome sequences. *J. Mol. Biol.* 428, 726–731. doi: 10.1016/j.jmb.2015.11.006

Kawasaki, A., Donn, S., Ryan, P. R., Mathesius, U., Devilla, R., Jones, A., et al. (2016). Microbiome and exudates of the root and rhizosphere of *Brachypodium distachyon*, a model for wheat. *PLoS One* 11:e0164533. doi: 10.1371/journal.pone.0164533

Kimotho, R. N., and Maina, S. (2024). Unraveling plant-microbe interactions: can integrated omics approaches offer concrete answers? *J. Exp. Bot.* 75, 1289–1313. doi: 10.1093/jxb/erad448

Kosar, F., Akram, N. A., Sadiq, M., Al-Qurainy, F., and Ashraf, M. (2018). Trehalose: a key organic osmolyte effectively involved in plant abiotic stress tolerance. *J. Plant Growth Regul.* 38:1. doi: 10.1007/s00344-018-9876-x

Layeghifard, M., Hwang, D. M., and Guttman, D. S. (2017). Disentangling interactions in the microbiome: A network perspective. *Trends Microbiol.* 217–28. doi: 10.1016/j.tim.2016.11.008

Letunic, I., and Bork, P. (2007). Interactive tree of life (iTOL): an online tool for phylogenetic tree display and annotation. *Bioinformatics* 23, 127–128. doi: 10.1093/bioinformatics/btl529

Li, Z., Chang, S., Lin, L., Li, Y., and An, Q. (2011). A colorimetric assay of 1-aminocyclopropane-1-carboxylate (ACC) based on ninhydrin reaction for rapid screening of bacteria containing ACC deaminase. *Lett. Appl. Microbiol.* 53, 178–185. doi: 10.1111/j.1472-765X.2011.03088.x

Li, M., Kennedy, A., Huybrechts, M., Dochy, N., and Geuten, K. (2019). The effect of ambient temperature on *Brachypodium distachyon* development. *Front. Plant Sci.* 10:1011. doi: 10.3389/fpls.2019.01011

Lin, H., and Peddada, S. D. (2020). Analysis of compositions of microbiomes with bias correction. *Nat. Commun.* 11:3514. doi: 10.1038/s41467-020-17041-7

Liu, Y.-X., Qin, Y., and Bai, Y. (2019). Reductionist synthetic community approaches in root microbiome research. *Curr. Opin. Microbiol.* 49, 97–102. doi: 10.1016/j.mib.2019.10.010

Liu, Y.-X., Qin, Y., Chen, T., Lu, M., Qian, X., Guo, X., et al. (2021). A practical guide to amplicon and metagenomic analysis of microbiome data. *Protein Cell* 12, 315–330. doi: 10.1007/s13238-020-00724-8

Louca, S., Polz, M. F., Mazel, F., Albright, M. B. N., Huber, J. A., O'Connor, M. I., et al. (2018). Function and functional redundancy in microbial systems. *Nat. Ecol. Evol.* 2, 936–943. doi: 10.1038/s41559-018-0519-1

Louden, B. C., Haarmann, D., and Lynne, A. M. (2011). Use of blue agar CAS assay for siderophore detection. *J. Microbiol. Biol. Educ.* 12, 51–53. doi: 10.1128/jmbe.v12i1.249

Martins, S. J., Pasche, J., Silva, H. A. O., Selten, G., Savastano, N., Abreu, L. M., et al. (2023). The use of synthetic microbial communities to improve plant health. *Phytopathology.* 8, 1369–1379. doi: 10.1094/PHYTO-01-23-0016-IA

McCarty, N. S., and Ledesma-Amaro, R. (2019). Synthetic biology tools to engineer microbial communities for biotechnology. *Trends Biotechnol.* 37, 181–197. doi: 10.1016/j.tibtech.2018.11.002

Mendes, R., Garbeva, P., and Raaijmakers, J. M. (2013). The rhizosphere microbiome: significance of plant beneficial, plant pathogenic, and human pathogenic microorganisms. *FEMS Microbiol. Rev.* 37, 634–663. doi: 10.1111/1574-6976.12028

Ngumbi, E., and Kloepper, J. (2016). Bacterial-mediated drought tolerance: current and future prospects. *Appl. Soil Ecol.* 105, 109–125. doi: 10.1016/j.apsoil.2016.04.009

Nordstedt, N. P., Roman-Reyna, V., Jacobs, J. M., and Jones, M. L. (2021). Comparative genomic understanding of gram-positive plant growth-promoting *Leifsonia*. *Phytobiomes J.* 5, 263–274. doi: 10.1094/PBIOMES-12-20-0092-SC

Novak, V., Andeer, P. F., Bowen, B. P., Ding, Y., Zhalnina, K., Hofmockel, K. S., et al. (2024). Reproducible growth of Brachypodium in EcoFAB 2.0 reveals that nitrogen form and starvation modulate root exudation. *Sci. Adv.* 10:eadg7888. doi: 10.1126/sciadv.adg7888

O'Banion, B. S., O'Neal, L., Alexandre, G., and Lebeis, S. L. (2020). Bridging the gap between single-strain and community-level plant-microbe chemical interactions. *Mol. Plant-Microbe Interact.* 33, 124–134. doi: 10.1094/MPMI-04-19-0115-CR

Olanrewaju, O. S., Ayilara, M. S., Ayangbenro, A. S., and Babalola, O. O. (2021). Genome mining of three plant growth-promoting *Bacillus* species from maize rhizosphere. *Appl. Biochem. Biotechnol.* 193, 3949–3969. doi: 10.1007/s12010-021-03660-3

Ong, K. S., Aw, Y. K., Lee, L. H., Yule, C. M., Cheow, Y. L., and Lee, S. M. (2016). *Burkholderia paludis* sp. nov., an antibiotic-siderophore producing novel *Burkholderia cepacia* complex species, isolated from Malaysian tropical peat swamp soil. *Front. Microbiol.* 7:2046. doi: 10.3389/fmicb.2016.02046

Orimoloye, I. R. (2022). Agricultural drought and its potential impacts: enabling decision-support for food security in vulnerable regions. *Frontiers in Sustainable Food Systems*, 6:838824. doi: 10.3389/fsufs.2022.838824

Orozco-Mosqueda, M. D. C., Glick, B. R., and Santoyo, G. (2020). ACC deaminase in plant growth-promoting bacteria (PGPB): an efficient mechanism to counter salt stress in crops. *Microbiol. Res.* 235:126439. doi: 10.1016/j.micres.2020.126439

Parks, D. H., Chuvochina, M., Rinke, C., Mussig, A. J., Chaumeil, P.-A., and Hugenholtz, P. (2022). GTDB: an ongoing census of bacterial and archaeal diversity through a phylogenetically consistent, rank normalized and complete genome-based taxonomy. *Nucleic Acids Res.* 50, D785–D794. doi: 10.1093/nar/gkab776

Parks, D. H., Imelfort, M., Skennerton, C. T., Hugenholtz, P., and Tyson, G. W. (2015). CheckM: assessing the quality of microbial genomes recovered from isolates, single cells, and metagenomes. *Genome Res.* 25, 1043–1055. doi: 10.1101/gr.186072.114

Pascale, A., Proietti, S., Pantelides, I. S., and Stringlis, I. A. (2019). Modulation of the root microbiome by plant molecules: the basis for targeted disease suppression and plant growth promotion. *Front. Plant Sci.* 10:1741. doi: 10.3389/fpls.2019.01741

Pérez-Miranda, S., Cabirol, N., George-Téllez, R., Zamudio-Rivera, L. S., and Fernández, F. J. (2007). O-CAS, a fast and universal method for siderophore detection. *J. Microbiol. Methods* 70, 127–131. doi: 10.1016/j.mimet.2007.03.023

Peschel, S., Müller, C. L., Von Mutius, E., Boulesteix, A. L., and Depner, M. (2021). NetCoMi: network construction and comparison for microbiome data in R. *Briefings in Bioinformatics*, 22:bbaa290. doi: 10.1093/bib/bbaa290

Platamone, G., Procacci, S., Maccioni, O., Borromeo, I., Rossi, M., Bacchetta, L., et al. (2023). *Arthrobacter* sp. inoculation improves cactus pear growth, quality of fruits, and nutraceutical properties of cladodes. *Curr. Microbiol.* 80:266. doi: 10.1007/s00284-023-03368-z

Pradhan, S., Tyagi, R., and Sharma, S. (2022). Combating biotic stresses in plants by synthetic microbial communities: principles, applications and challenges. *J. Appl. Microbiol.* 133, 2742–2759. doi: 10.1111/jam.15799

Price, M. N., Dehal, P. S., and Arkin, A. P. (2009). Fasttree: computing large minimum evolution trees with profiles instead of a distance matrix. *Mol. Biol. Evol.* 26, 1641–1650. doi: 10.1093/molbev/msp077

Prjibelski, A., Antipov, D., Meleshko, D., Lapidus, A., and Korobeynikov, A. (2020). Using SPAdes de novo assembler. *Curr. Protoc. Bioinformatics* 70:e102. doi: 10.1002/cpbi.102

Pruesse, E., Peplies, J., and Glöckner, F. O. (2012). SINA: accurate high-throughput multiple sequence alignment of ribosomal RNA genes. *Bioinformatics* 28, 1823–1829. doi: 10.1093/bioinformatics/bts252

Qi, M., Berry, J. C., Veley, K. M., O'Connor, L., Finkel, O. M., Salas-González, I., et al. (2022). Identification of beneficial and detrimental bacteria impacting sorghum responses to drought using multi-scale and multi-system microbiome comparisons. *ISME J.* 16, 1957–1969. doi: 10.1038/s41396-022-01245-4

Quast, C., Pruesse, E., Yilmaz, P., Gerken, J., Schweer, T., Yarza, P., et al. (2013). The SILVA ribosomal RNA gene database project: improved data processing and web-based tools. *Nucleic Acids Res.* 41, D590–D596. doi: 10.1093/nar/gks1219

Rodríguez Amor, D., and Dal Bello, M. (2019). Bottom-up approaches to synthetic cooperation in microbial communities. *Life* 9:22. doi: 10.3390/life9010022

Rolli, E., Marasco, R., Vigani, G., Ettoumi, B., Mapelli, F., Deangelis, M. L., et al. (2015). Improved plant resistance to drought is promoted by the root-associated microbiome as a water stress-dependent trait. *Environ. Microbiol.* 17, 316–331. doi: 10.1111/1462-2920.12439

Sanchez-Gorostiaga, A., Bajić, D., Osborne, M. L., Poyatos, J. F., and Sanchez, A. (2018). High-order interactions dominate the functional landscape of microbial consortia. *BioRxiv.* doi: 10.1101/333534

Santos-Medellín, C., Edwards, J., Liechty, Z., Nguyen, B., and Sundaresan, V. (2017). Drought stress results in a compartment-specific restructuring of the rice root-associated microbiomes. *MBio* 8, 10–1128. doi: 10.1128/mBio.00764-17

Schimel, J., Balser, T. C., and Wallenstein, M. (2007). Microbial stress-response physiology and its implications for ecosystem function. *Ecology* 88, 1386–1394. doi: 10.1890/06-0219

Schmitz, L., Yan, Z., Schneijderberg, M., de Roij, M., Pijnenburg, R., Zheng, Q., et al. (2022). Synthetic bacterial community derived from a desert rhizosphere confers salt stress resilience to tomato in the presence of a soil microbiome. *ISME J.* 16, 1907–1920. doi: 10.1038/s41396-022-01238-3

Seleiman, M. F., Al-Suhaibani, N., Ali, N., Akmal, M., Alotaibi, M., Refay, Y., et al. (2021). Drought stress impacts on plants and different approaches to alleviate its adverse effects. *Plants* 10:259. doi: 10.3390/plants10020259

Shaffer, M., Borton, M. A., McGivern, B. B., Zayed, A. A., La Rosa, S. L., Solden, L. M., et al. (2020). DRAM for distilling microbial metabolism to automate the curation of microbiome function. *Nucleic Acids Res.* 48, 8883–8900. doi: 10.1093/nar/gkaa621

Sharma, M. P., Grover, M., Chourasiya, D., Bharti, A., Agnihotri, R., Maheshwari, H. S., et al. (2020). Deciphering the role of trehalose in tripartite symbiosis among rhizobia, arbuscular mycorrhizal fungi, and legumes for enhancing abiotic stress tolerance in crop plants. *Front. Microbiol.* 11:509919. doi: 10.3389/fmicb.2020.509919

Shayanthan, A., Ordoñez, P. A. C., and Oresnik, I. J. (2022). The role of synthetic microbial communities (syncom) in sustainable agriculture. *Front. Agron.* 4:896307. doi: 10.3389/fagro.2022.896307

Shi, H., Ye, T., Song, B., Qi, X., and Chan, Z. (2015). Comparative physiological and metabolomic responses of four *Brachypodium distachyon* varieties contrasting in drought stress resistance. *Acta Physiol. Plant.* 37:122. doi: 10.1007/s11738-015-1873-0

Sievers, F., Wilm, A., Dineen, D., Gibson, T. J., Karplus, K., Li, W., et al. (2011). Fast, scalable generation of high-quality protein multiple sequence alignments using Clustal omega. *Mol. Syst. Biol.* 7:539. doi: 10.1038/msb.2011.75

Sinsabaugh, F. (2001). Activity profiles of bacterioplankton in a eutrophic river. *Freshwater Biology* 46, 1239–1249. doi: 10.1046/j.1365-2427.2001.00748.x

Skalska, A., Beckmann, M., Corke, F., Savas Tuna, G., Tuna, M., Doonan, J. H., et al. (2021). Metabolomic variation aligns with two geographically distinct subpopulations of Brachypodium Distachyon before and after drought stress. *Cells* 10:683. doi: 10.3390/cells10030683

Sun, T., Liu, H., Wang, N., Huang, M., Banerjee, S., Jousset, A., et al. (2025). Interactions with native microbial keystone taxa enhance the biocontrol efficiency of *Streptomyces*. *Microbiome* 13:126. doi: 10.1186/s40168-025-02120-y

Toju, H., Abe, M. S., Ishii, C., Hori, Y., Fujita, H., and Fukuda, S. (2020). Scoring species for synthetic community design: network analyses of functional core microbiomes. *Front. Microbiol.* 11:1361. doi: 10.3389/fmicb.2020.01361

Tp, H. (2023). Economic impact of drought on agrarian society: the case study of a village in Maharashtra, India. *Int. J. Disaster Risk Reduct.* 96:103912. doi: 10.1016/j.ijdrr.2023.103912

Vives-Peris, V., de Ollas, C., Gómez-Cadenas, A., and Pérez-Clemente, R. M. (2020). Root exudates: from plant to rhizosphere and beyond. *Plant Cell Rep.* 39, 3–17. doi: 10.1007/s00299-019-02447-5

Voges, M. J. E. E. E., Bai, Y., Schulze-Lefert, P., and Sattely, E. S. (2019). Plant-derived coumarins shape the composition of an Arabidopsis synthetic root microbiome. *Proc. Natl. Acad. Sci. USA* 116, 12558–12565. doi: 10.1073/pnas.1820691116

Vorholt, J. A., Vogel, C., Carlström, C. I., and Müller, D. B. (2017). Establishing causality: opportunities of synthetic communities for plant microbiome research. *Cell Host Microbe* 22, 142–155. doi: 10.1016/j.chom.2017.07.004

Wei, S., Jacquiod, S., Philippot, L., Blouin, M., and Sørensen, S. J. (2021). Spatial analysis of the root system coupled to microbial community inoculation shed light on rhizosphere bacterial community assembly. *Biol. Fertil. Soils* 57, 973–989. doi: 10.1007/s00374-021-01590-0

Werner, G. D. A., and Kiers, E. T. (2015). Order of arrival structures arbuscular mycorrhizal colonization of plants. *New Phytol.* 205, 1515–1524. doi: 10.1111/nph.13092

Xia, M., Chakraborty, R., Terry, N., Singh, R. P., and Fu, D. (2020). Promotion of saltgrass growth in a saline petroleum hydrocarbons contaminated soil using a plant growth promoting bacterial consortium. *Int. Biodeterior. Biodegrad.* 146:104808. doi: 10.1016/j.ibiod.2019.104808

Zegeye, E. K., Brislawn, C. J., Farris, Y., Fansler, S. J., Hofmockel, K. S., Jansson, J. K., et al. (2019). Selection, succession, and stabilization of soil microbial consortia. *mSystems* 4, 10–1128. doi: 10.1128/mSystems.00055-19

Zhalnina, K., Louie, K. B., Hao, Z., Mansoori, N., da Rocha, U. N., Shi, S., et al. (2018). Dynamic root exudate chemistry and microbial substrate preferences drive patterns in rhizosphere microbial community assembly. *Nat. Microbiol.* 3, 470–480. doi: 10.1038/s41564-018-0129-3

Zia, R., Nawaz, M. S., Siddique, M. J., Hakim, S., and Imran, A. (2021). Plant survival under drought stress: implications, adaptive responses, and integrated rhizosphere management strategy for stress mitigation. *Microbiol. Res.* 242:126626. doi: 10.1016/j.micres.2020.126626